A Search For 3-lepton Resonances In A Minimal SUSY B-L R-parity Violating Model

Jeff Dandoy, Ian Dyckes, Lucas Flores,
Leigh Schaefer, Evelyn Thomson

University Of Pennsylvania

July 12, 2021

Published!

PHYSICAL REVIEW D **103,** 112003 (2021)

Search for trilepton resonances from chargino and neutralino pair production in $\sqrt{s} = 13$ TeV pp collisions with the ATLAS detector

G. Aad *et al.*[*]
(ATLAS Collaboration)

(Received 23 November 2020; accepted 23 April 2021; published 7 June 2021)

- Analysis was published just recently on June 7th
  - https://journals.aps.org/prd/pdf/10.1103/PhysRevD.103.112003
- Can also view aux material here as well as in our HEPData space
  - https://www.hepdata.net/record/ins1831992

Minimal SUSY B-L Model

- SUSY introduces Baryon (**B**) and Lepton number (**L**) violating interactions
- Popular solution: "**R-parity**" ($R=(-1)^{3(B-L)+2s}$) conservation (RPC) which forbids B and L violation entirely
- RPC requires a stable, lightest SUSY particle → convenient dark matter candidate

  → However this solution is ad hoc
- Instead, we can add a gauged $U(1)_{B-L}$ symmetry (with right handed neutrinos) and get away with only violating lepton number a bit

  → consistent with proton stability and bounds on L violation
- Call this the ***Minimal SUSY B-L Model*** 1604.08588, 1501.01886, 1503.01473, 1811.05581

Search Motivation: Signals of Interest

- Theorists performed large statistical scan of SUSY initial parameters (10 million points)
  - LSP calculated for each point
- Wino **neutralino** (χ^0_W) and wino **chargino** ($\chi^\pm_W$) are have high LSP probability
- **Bino** (χ^0_B) production cross-section too low to be experimentally viable

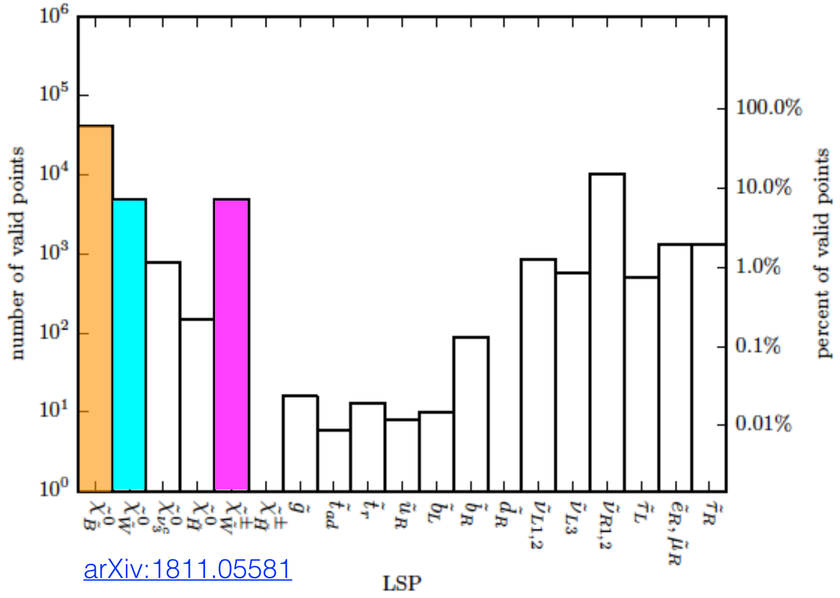

arXiv:1811.05581

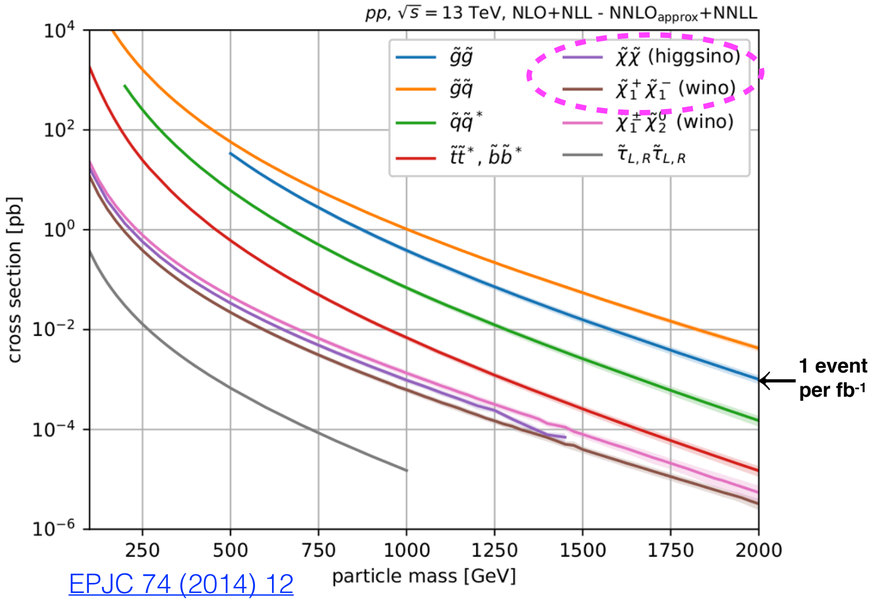

EPJC 74 (2014) 12

Signals of Interest

- With that we are considering both $\chi^{\pm}_{W}\chi^{\mp}_{W}$ and $\chi^{\pm}_{W}\chi^{0}_{W}$ production
- $\chi^{\pm}_{W}$ and χ^{0}_{W} are assumed to be mass degenerate and both decay via RPV (more in back-up)
- Will focus on $\chi^{\pm}_{W}\rightarrow Z\ell\rightarrow\ell\ell\ell$, giving us a **resonance in the trilepton invariant mass**
- χ^{0}_{W} decaying via RPV offers further discrimination power in $\chi^{\pm}_{W}\chi^{0}_{W}$ production
- A 3 lepton ***resonance*** search has not been done in by either CMS or ATLAS since Run 1 (1506.01291)

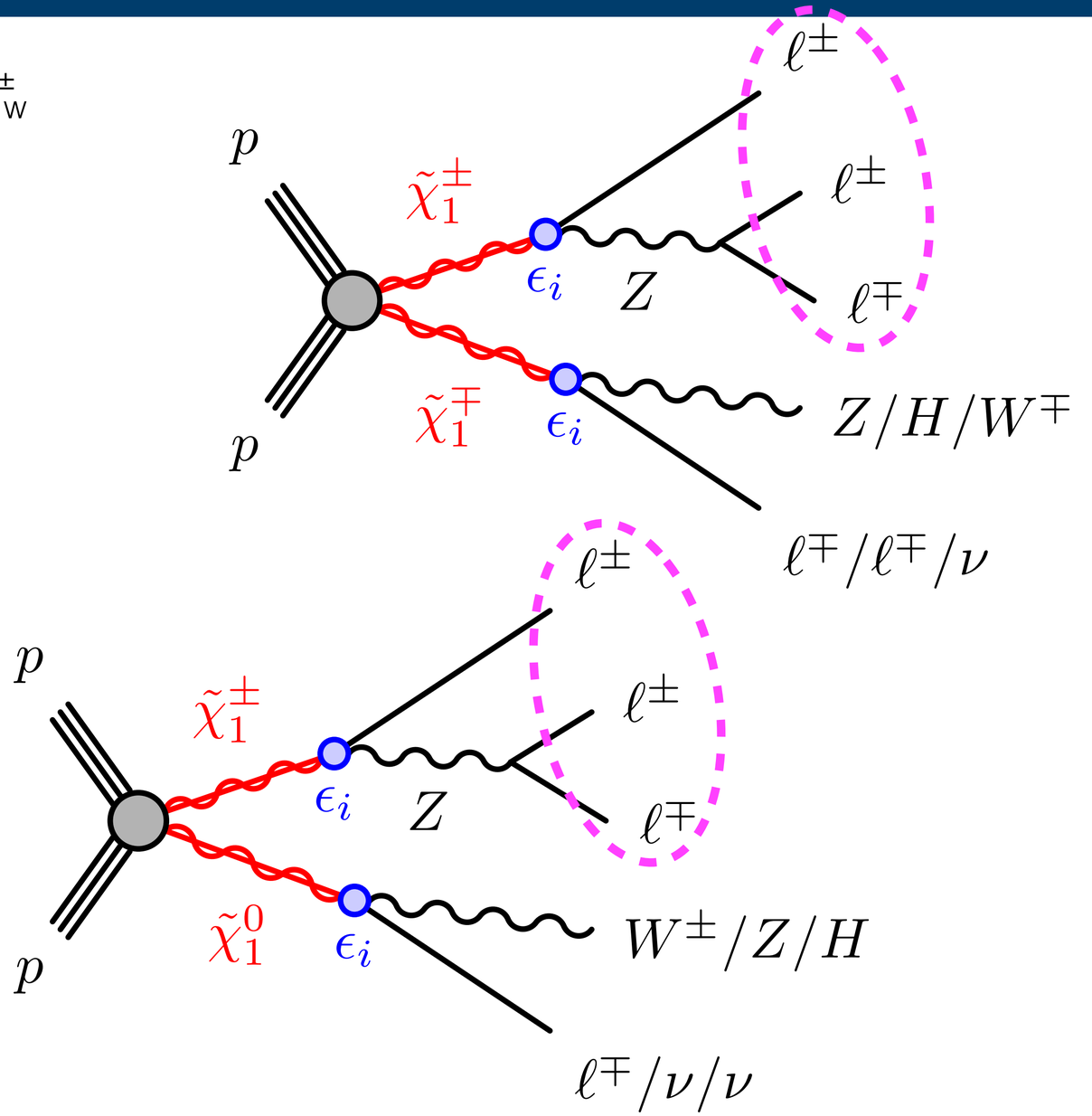

Signal Regions: Motivation

- Many final states possible
- Some fully visible and many with >3 leptons
- Design 3 search regions to target these different final states
- When other wino's decay is fully visible, fully reconstruct both winos
- When other wino decays semi-visibly, use extra leptons for discrimination with SM

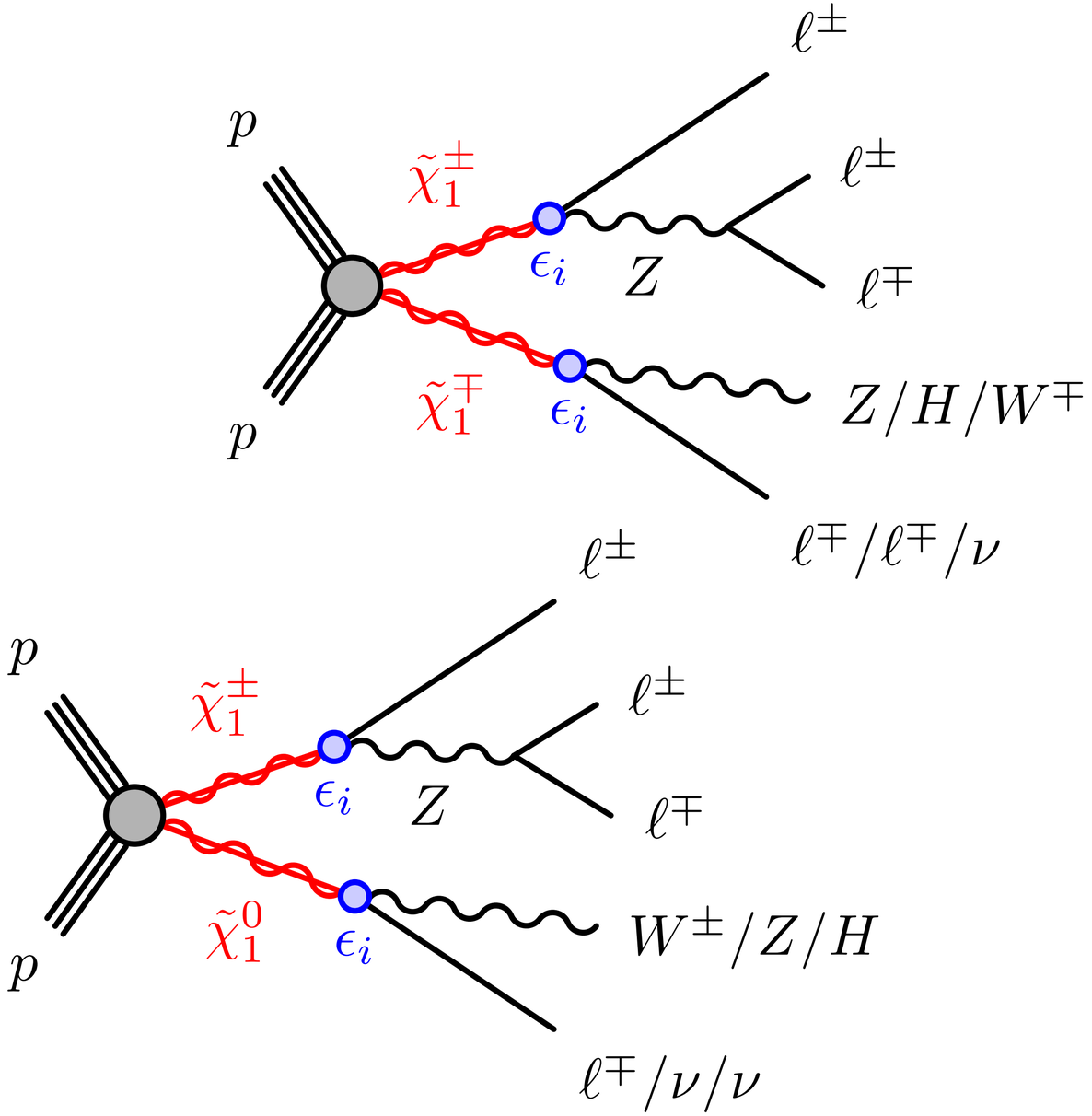

Signal Regions: Definitions

- **SR3ℓ**: 3 ℓeptons

  $m_{Z\ell}$ is the invariant mass of the only 3 leptons

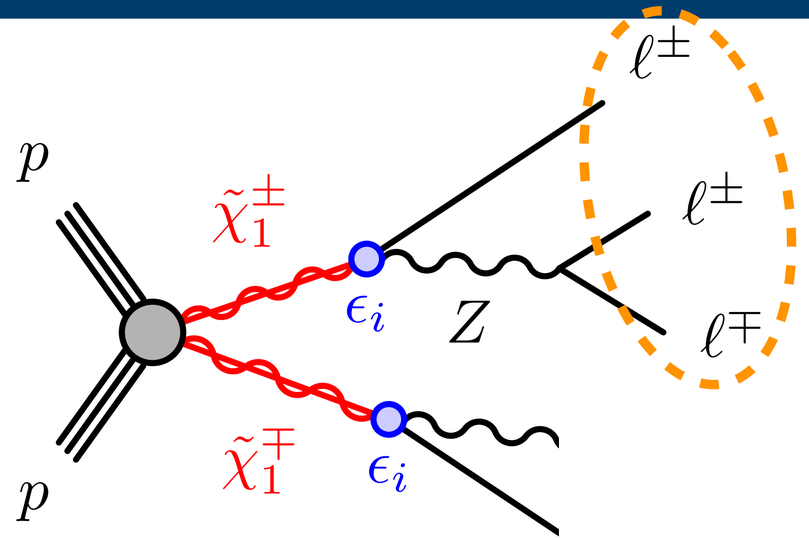

Signal Regions: Definitions

- SR3ℓ: 3 ℓeptons

  $m_{Z\ell}$ is the invariant mass of the only 3 leptons

- SR4ℓ: 4 ℓeptons

  4th lepton introduces ambiguity→ match using ΔR or max $m_{Z\ell}$ depending on energy

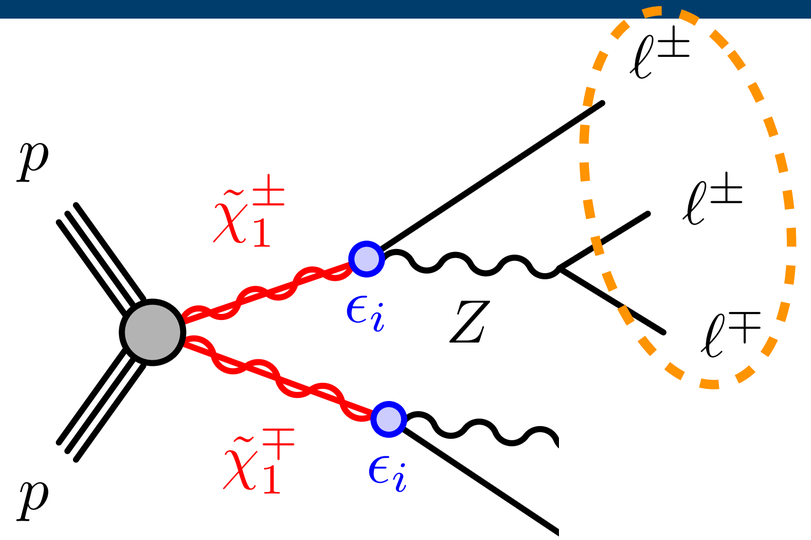

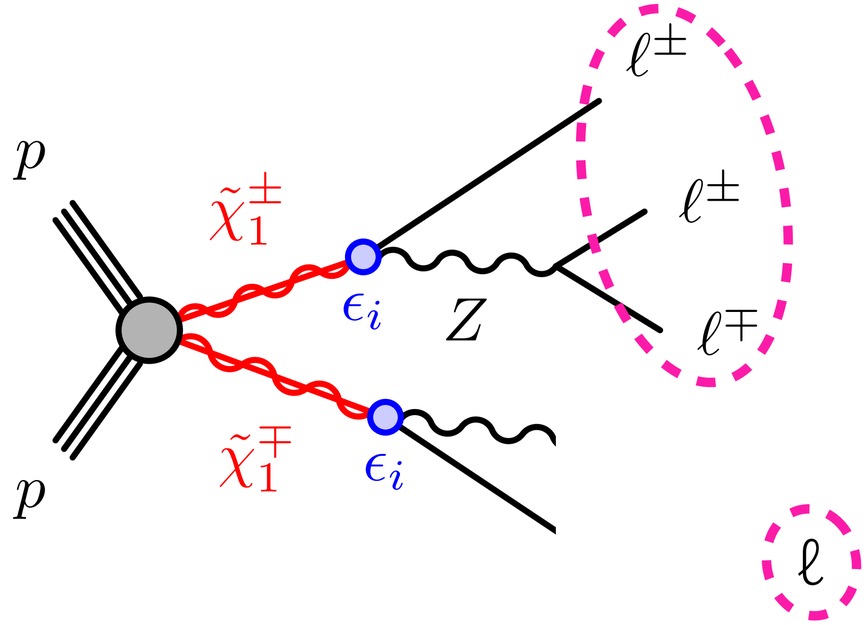

Signal Regions: Definitions

- **SR3ℓ**: 3 ℓeptons

  $m_{Z\ell}$ is the invariant mass of the only 3 leptons

- **SR4ℓ**: 4 ℓeptons

  4th lepton introduces ambiguity→ match using ΔR or max $m_{Z\ell}$ depending on energy

- **SRFR**: Fully Reconstructed

  Determine $m_{Z\ell}$ for each leg via minimizing

  ↓

$$m_{Z\ell}^{asym} = \frac{|m_{Z\ell_i} - m_{B\ell_j}|}{(m_{Z\ell_i} + m_{B\ell_j})}$$

  B=Boson

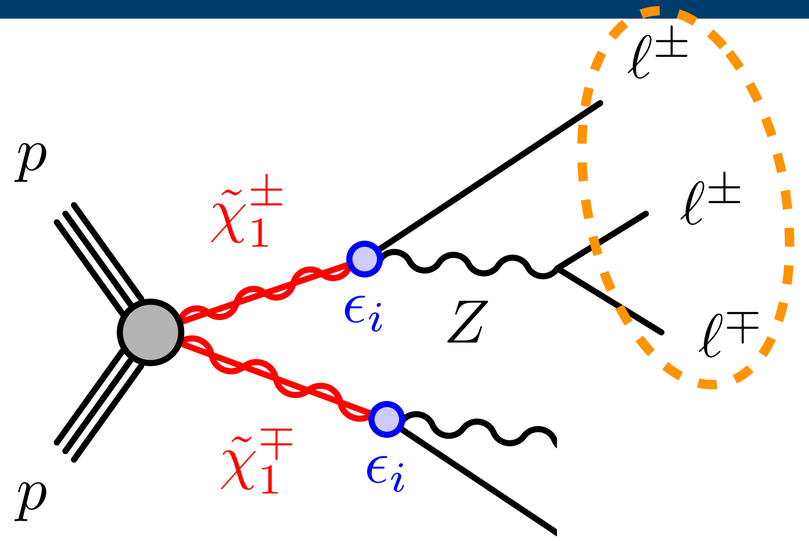

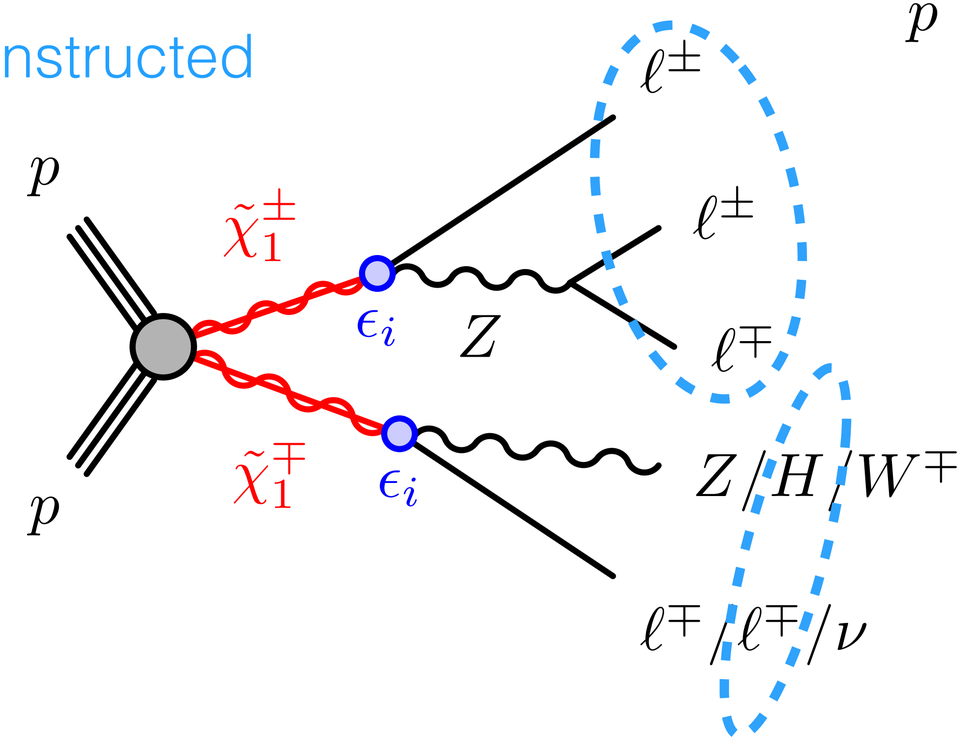

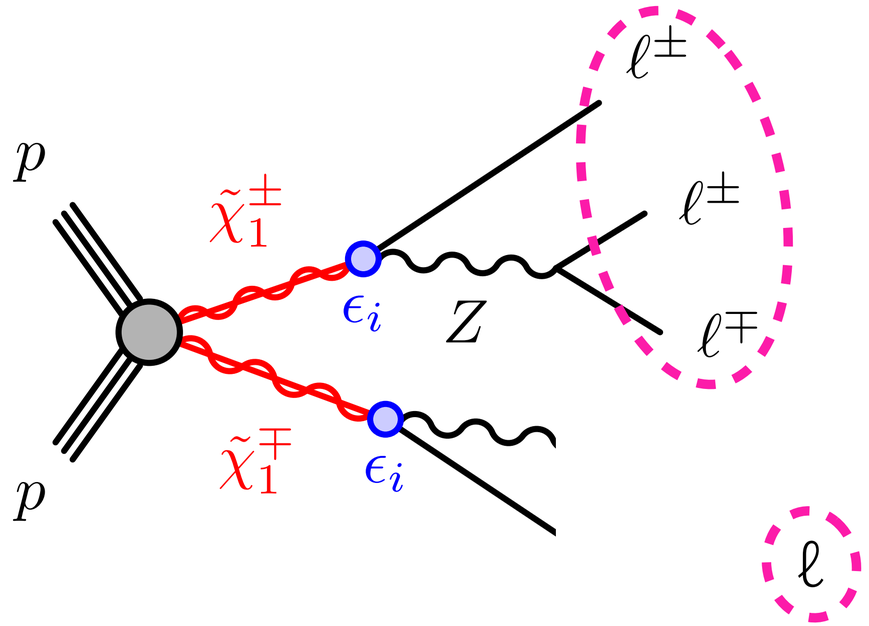

Background Estimation: Control and Validation Regions

- Dominant backgrounds are WZ, ZZ, and ttZ
- Design CRs and VRs to target these to better estimate their contributions
- Fake backgrounds are estimated using data-driven fake factor method
- Cartoons depict the carved out phase space of our regions, and how orthogonality is maintained
- Table and more details in back-up

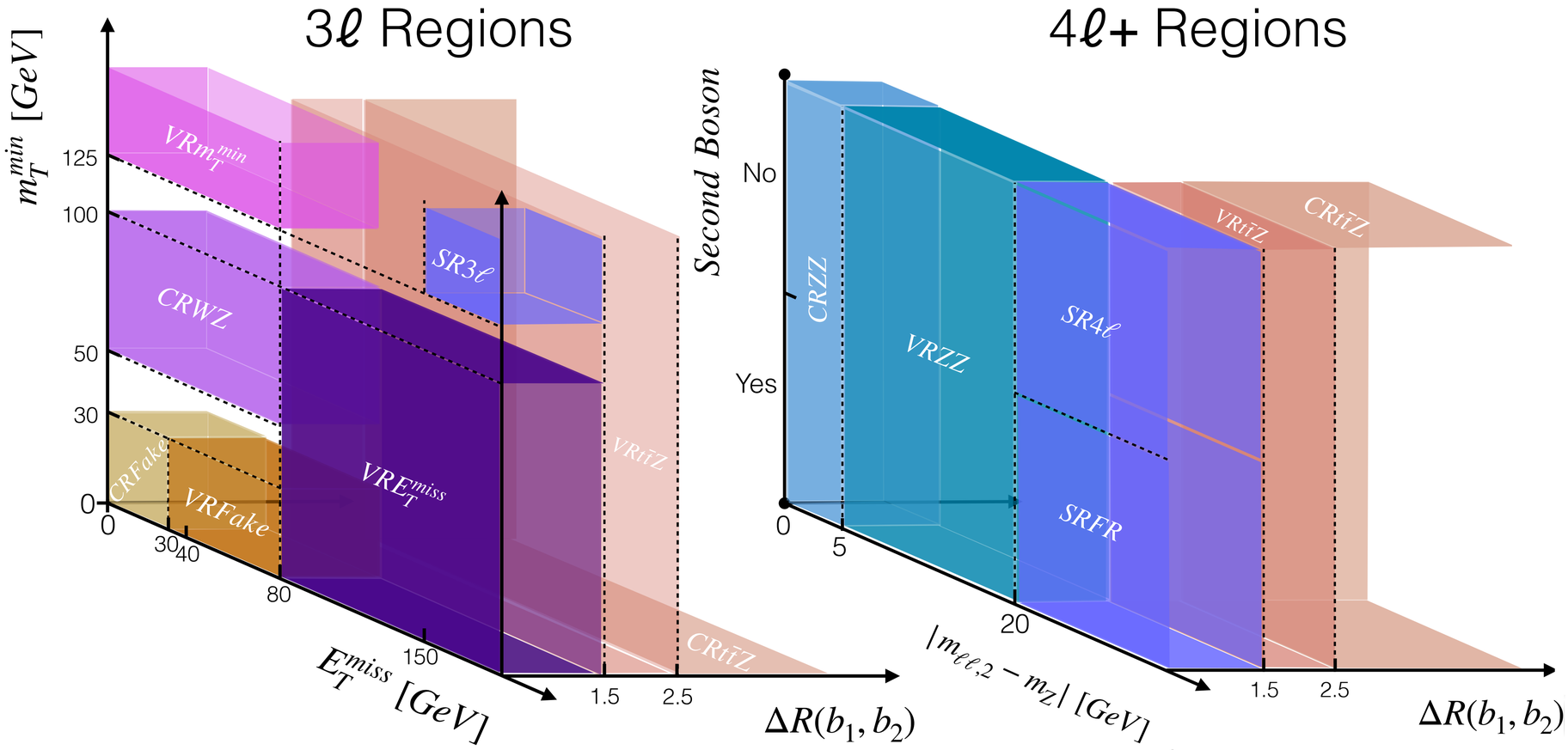

Background Estimation : Yields and Agreement

- SM backgrounds are normalized to data in dedicated Control Regions (CR) and checked in Validation Regions (VR) via fit based on a profile likelihood test statistic
- Top panel: Expected and observed yields in each CR and VR. Bottom panel: Significance of deviations between data and expectation
- Good data/MC agreement in VRs post fit
- VR pulls ~1.9σ or less.
- $m_{Z\ell}$ dists. checked in regions and shapes agree well (no features observed).

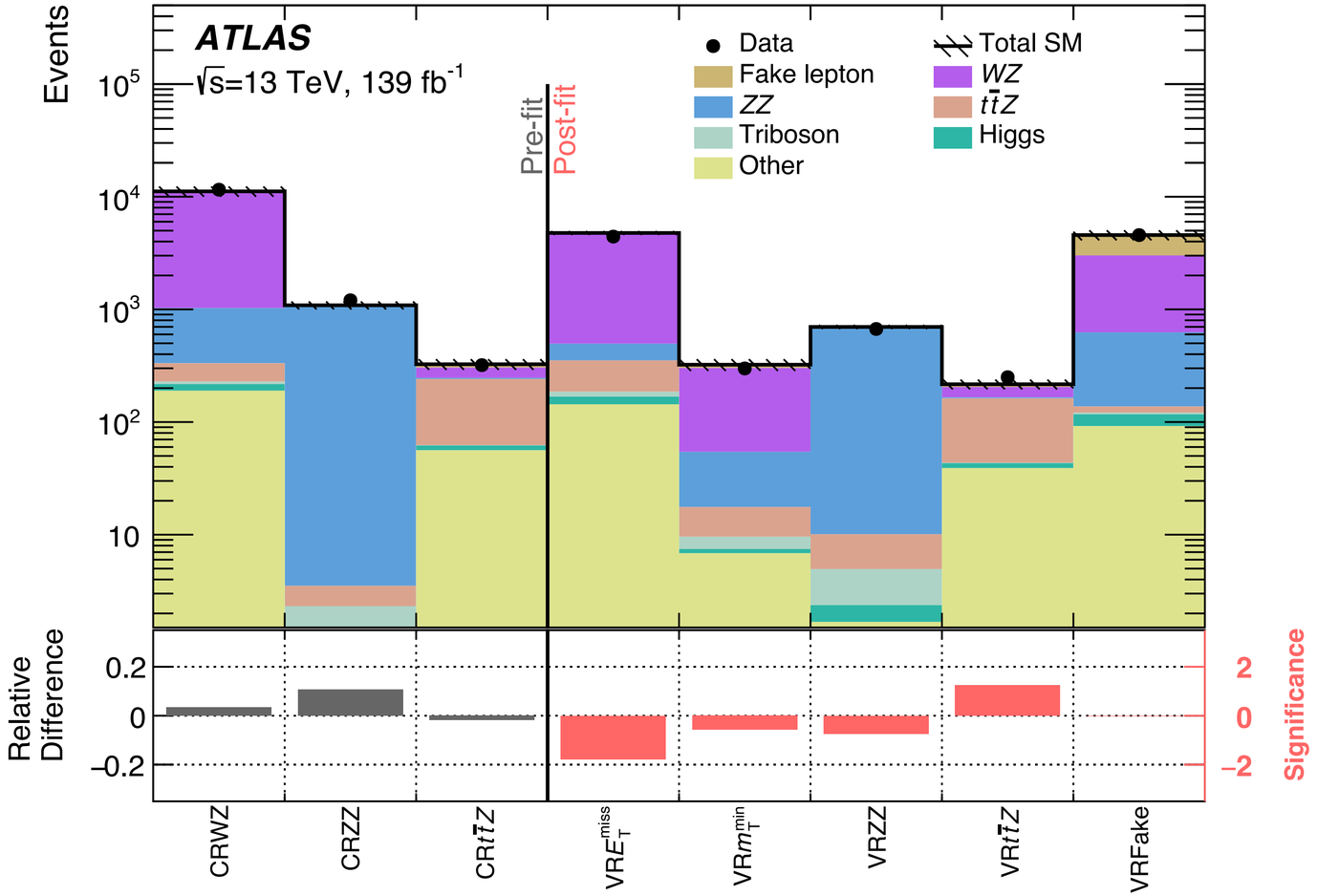

$$\mu_{WZ} = 1.01 \pm 0.03 \qquad \mu_{ZZ} = 1.12 \pm 0.06 \qquad \mu_{t\bar{t}Z} = 1.05 \pm 0.18$$

Results

- A simultaneous fit in $m_{Z\ell}$ among all 3 SRs is done
- Top panel: Expected and observed yields in each $m_{Z\ell}$ bin of each SR. Bottom panel: Significance of deviations between data and expectation
- Three example signal mass points overlaid
- SRs show good agreement in the shape of the $m_{Z\ell}$ distribution between data and the SM expectation, with no significant localized excesses.

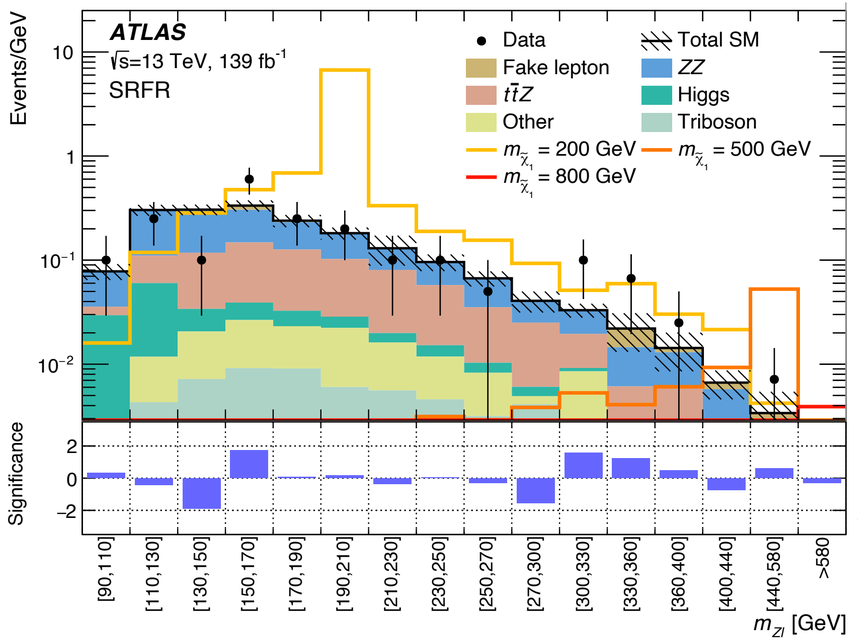

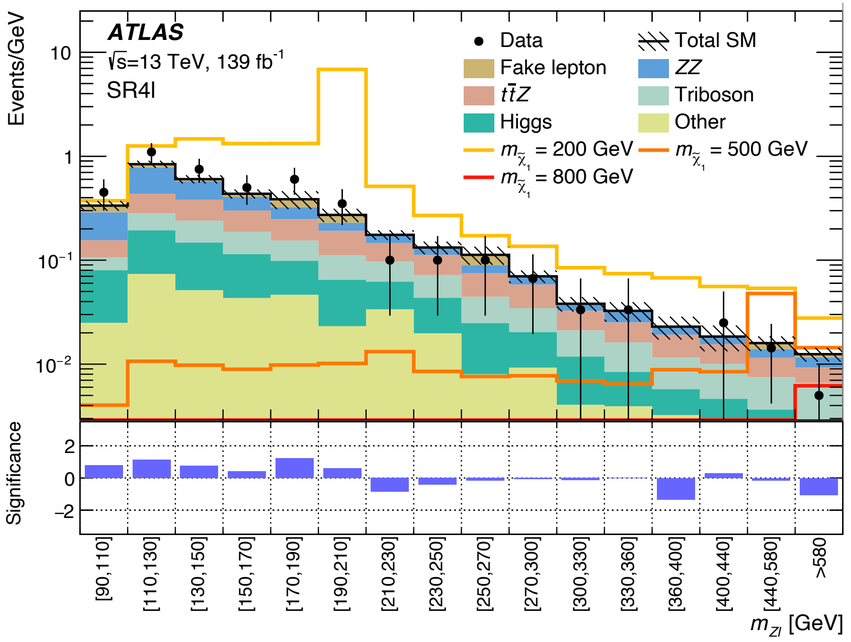

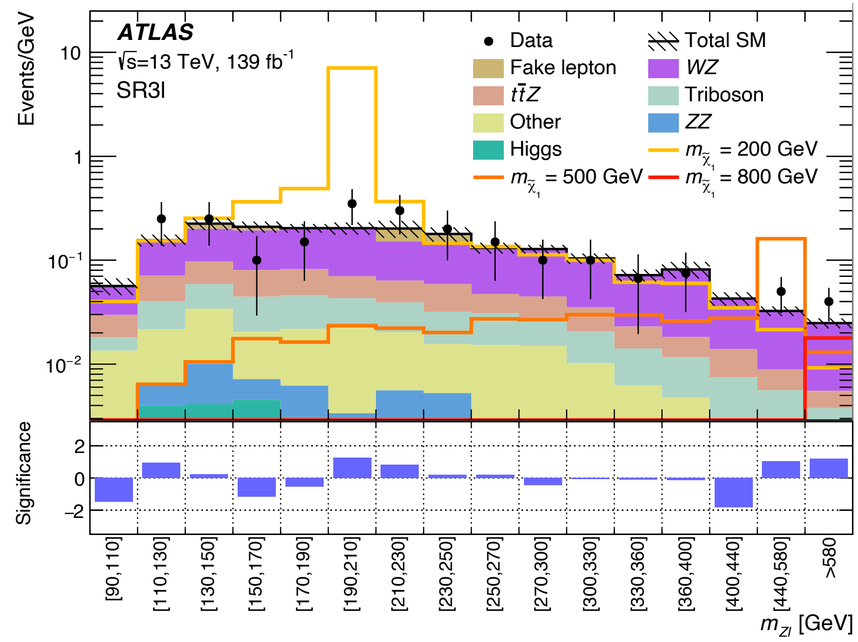

Setting Limits: Model Dependent

- Exclusion limits on the generated SUSY $\chi_1^{\pm}/\chi_1^0$ signal samples are derived at 95% confidence level through the profile log-likelihood ratio test using the CL_S prescription and performed with HistFitter.
- Each bin of the $m_{Z\ell}$ distribution in each SR is fit independently, so there are effectively 48 SRs being fit simultaneously
- The considered points in the lepton flavor scan are (BR($\chi_W \rightarrow Be$), BR($\chi_W \rightarrow B\,\mu$), BR($\chi_W \rightarrow B\,\tau$))= (1,0,0),(0,1,0),(0,0,1), and (0.33,0.33,0.33), where B is a W boson for the neutralino, and can be either a Z or a higgs for the chargino
- Then for each of these points, a finer granularity scan is performed over the BRs of the possible boson types of the wino decay

Setting Limits : Model Dependent

- Showing exclusions in the plane of the branching fraction for $\chi_1^\pm/\chi_1^0$ decays to Z(y-axis) and $\chi_1^\pm/\chi_1^0$ mass (x-axis)
- Limits are for combined $\chi_1^\pm\chi_1^\mp$ and $\chi_1^\pm\chi_1^0$ production
- Assume branching ratios of $\chi_1^\pm$ and χ_1^0 are fully correlated
- Direct lepton BR scanned

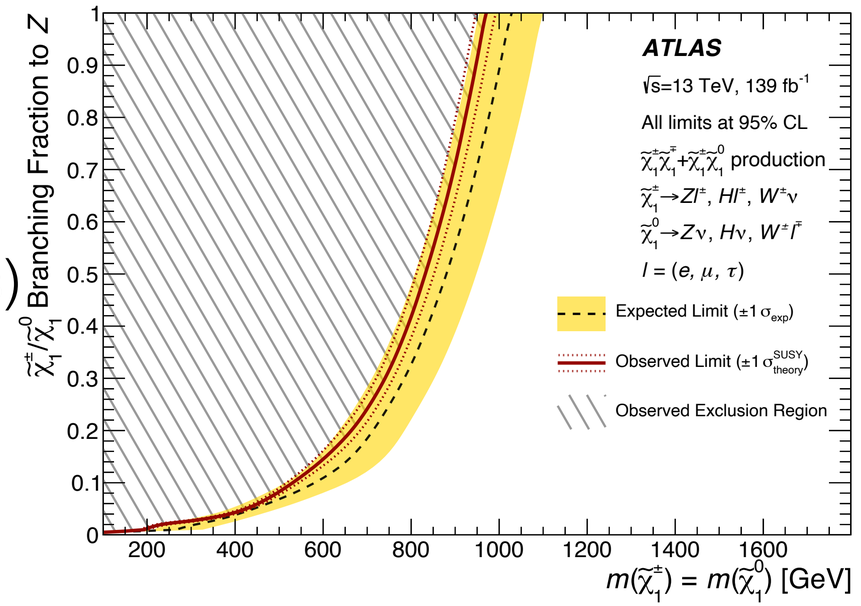

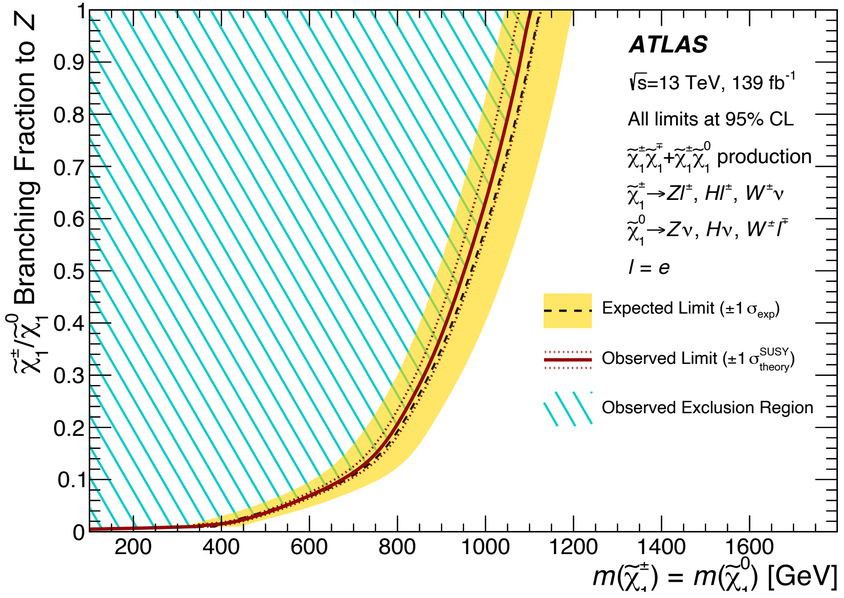

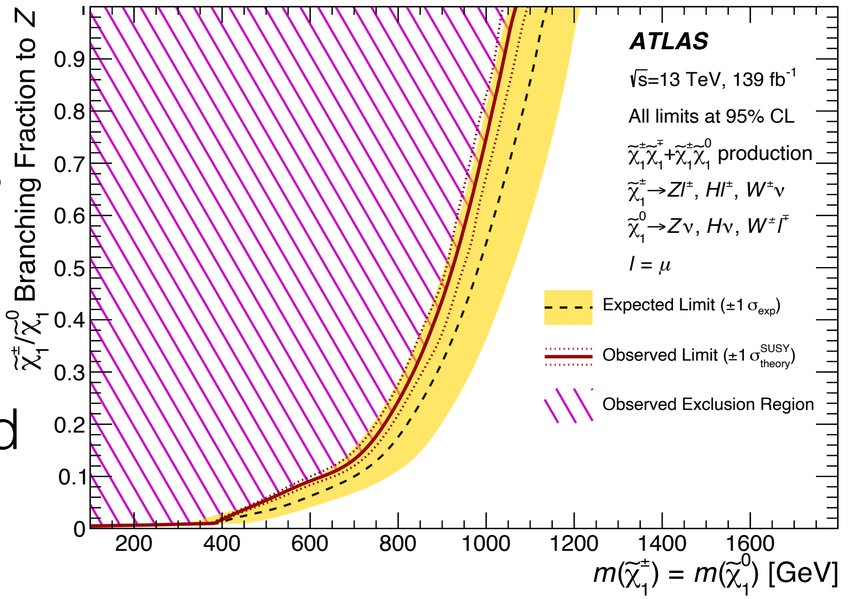

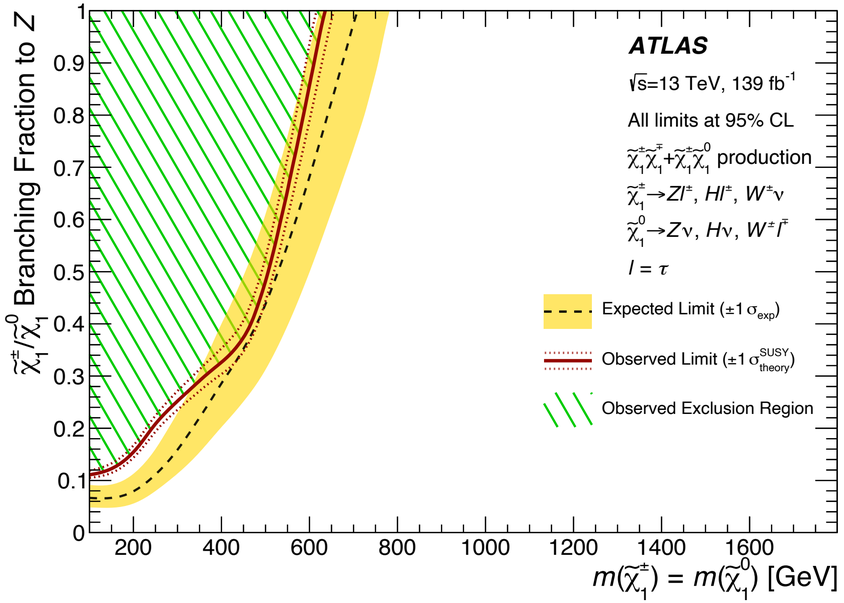

Setting Limits : Model Dependent

- Showing exclusions in the plane of the branching fraction for $\chi_1^\pm/\chi_1^0$ decays to Higgs (y-axis) and $\chi_1^\pm/\chi_1^0$ decays to Z (x-axis)
- Limits are for combined $\chi_1^\pm\chi_1^\mp$ and $\chi_1^\pm\chi_1^0$ production
- Assume branching ratios of $\chi_1^\pm$ and χ_1^0 are fully correlated
- Direct lepton BR scanned

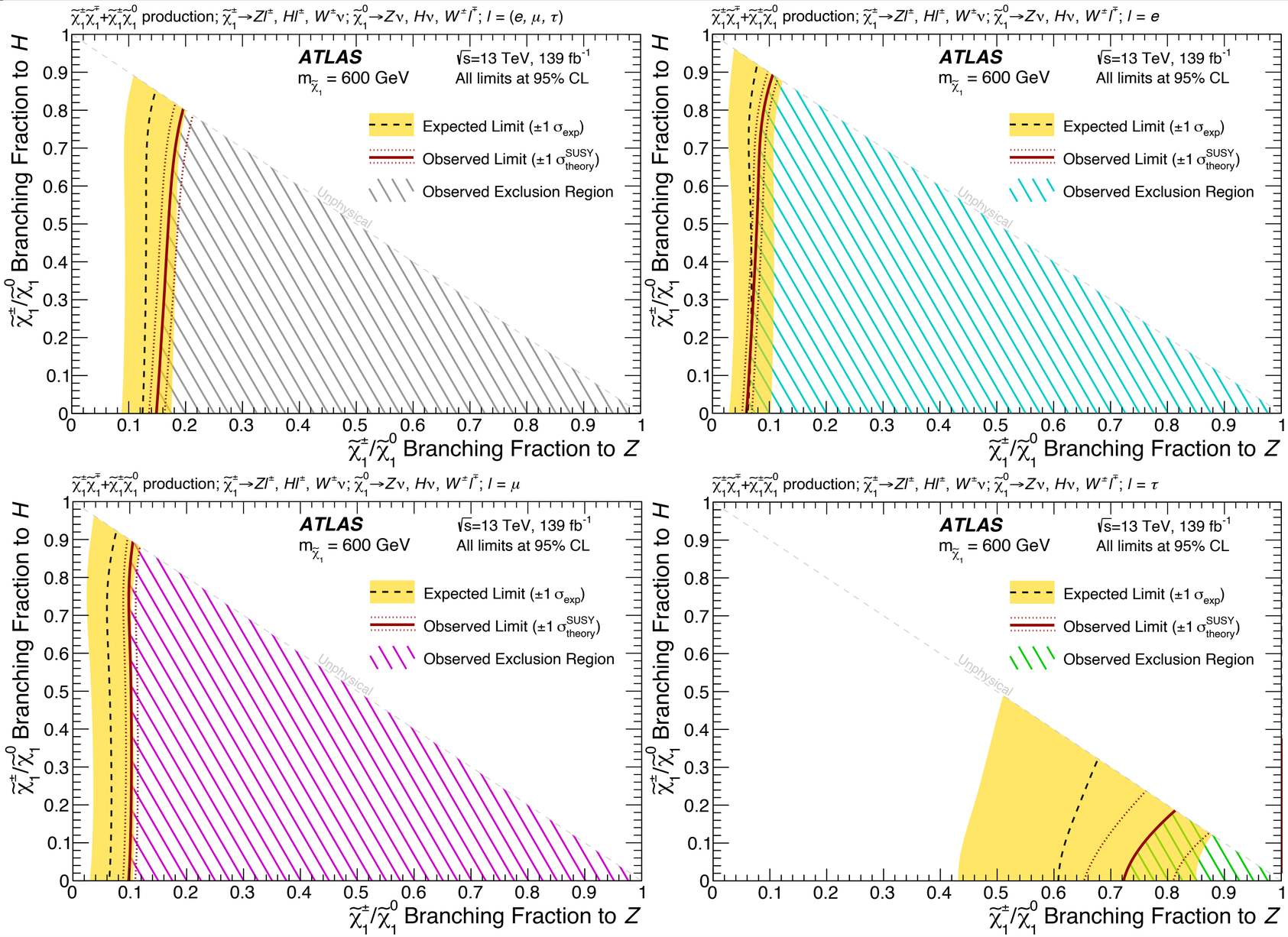

Summary and Conclusion

- A search was done for a trilepton resonance in 139 fb^{-1} of proton-proton collision data collected at ATLAS
- No significant excess was seen
- Model independent limits were set as well as model dependent limits in the mass-BR(Z) and BR(Z)-BR(H) planes
- Current feasibility studies being done for a new analysis focusing on a $\chi^{\pm}_{W} \rightarrow H\ell \rightarrow bb\ell$ resonance using large R jets

Thanks!

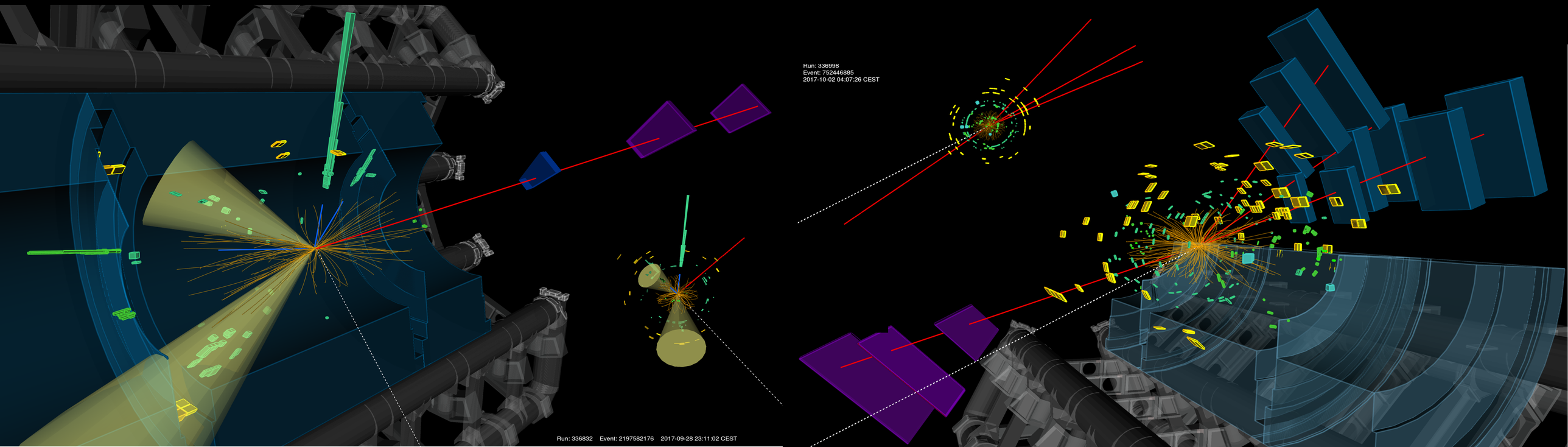
Run: 336998
Event: 752446885
2017-10-02 04:07:26 CEST
Run: 336832 Event: 2197582176 2017-09-28 23:11:02 CEST

back up

Background Estimation: Control and Validation Regions

N leptons	3	4
Prompt	WZ, ttZ	ZZ, ttZ, Higgs
Fake	Zjets, top	WZ, top

- Dominant SM and fake backgrounds change depending on lepton multiplicity
- Dominant backgrounds are WZ, ZZ, and ttZ
- Design CRs and VRs to target these to better estimate their contributions
  - WZ: Require 3 leptons. Cuts on E_T^{miss} and m_T^{min}
  - ttZ: Cuts on E_T^{miss}, n-bjets≥2 (back-to-back $\Delta R(b_0,b_1)$)
  - ZZ: Require two Zs (four leptons)
- Fake backgrounds are estimated using data-driven fake factor method
  - → Systematic accounts for several sources and compositions
  - → Z+jets CR and VR also used for fake factor measurement

Background Estimation: Control and Validation Regions

- Or if you prefer a classic table…

Region	N_{lep}	$E_{\text{T}}^{\text{miss}}$ [GeV]	$m_{\text{T}}^{\text{min}}$ [GeV]	Second boson	Second leptonic Z; $\lvert m_{\ell\ell,2} - m_Z \rvert$ [GeV]	$N_{b\text{-jet}}$	$\Delta R(b_1, b_2)$	$m_{Z\ell}^{\text{asym}}$
SRFR	≥4	···	···	Yes	Veto; <20	···	<1.5	<0.1
SR4ℓ	≥4	>80*	···	No	Veto; <20	···	<1.5	···
CRZZ	=4	···	···	···	Require; <5	···	<1.5	···
VRZZ	=4	···	···	···	Require; [5, 20]	···	<1.5	···
CR$t\bar{t}Z$	≥3	>40	···	···	Veto; <20	≥2	>2.5	···
VR$t\bar{t}Z$	≥3	>40	···	···	Veto; <20	≥2	[1.5, 2.5]	···
SR3ℓ	=3	>150	>125	···	···	···	<1.5	···
CRWZ	=3	<80	[50, 100]	···	···	···	<1.5	···
VR$E_{\text{T}}^{\text{miss}}$	=3	>80	<100	···	···	···	<1.5	···
VR$m_{\text{T}}^{\text{min}}$	=3	<80	>125	···	···	···	<1.5	···
CRFake	=3	<30	<30	···	···	···	<1.5	···
VRFake	=3	[30, 80]	<30	···	···	···	<1.5	···

Statistical Treatment

- A fit based on a profile likelihood test statistic is performed on all CRs and SRs simultaneously using the HistFitter package to estimate the final postfit background prediction and uncertainty
- Binning in the primary discriminating variable, $m_{Z\ell}$, is optimized for signal sensitivity and the variable binning below is used

$$m_{Z\ell} = 90,110,130,150,170,190,210,230,250,270,300,330,360,400,440, \text{ and } 580\ GeV$$

  - This effectively gives us $(3$ SRs $\times\ 16\ m_{Z\ell}$ bins$) = 48$ independent SRs to fit simultaneously

Results

- Inclusive and by-flavor observed and expected yields
- Regions with a lepton subscript are yields determined from a fit requiring the direct non-Z lepton to be that specified flavor

Region	SRFR	$SRFR_e$	$SRFR_\mu$	$SR4\ell$	$SR4\ell_e$	$SR4\ell_\mu$
Observed yield	42	15	17	89	48	41
Expected background yield	39 ± 4	13.7 ± 2.0	15.7 ± 2.5	76 ± 6	35.8 ± 3.5	38.2 ± 2.8
WZ yield	...	...	...	...	...	...
ZZ yield	19 ± 4	7.1 ± 1.7	10.4 ± 2.4	20.9 ± 1.1	9.5 ± 0.6	11.2 ± 0.7
$t\bar{t}Z$ yield	12.2 ± 3.2	2.4 ± 0.7	3.0 ± 0.6	18 ± 6	9.1 ± 3.2	8.5 ± 1.6
Triboson yield	1.3 ± 0.4	0.25 ± 0.09	0.33 ± 0.12	12.2 ± 2.8	5.8 ± 1.4	6.0 ± 1.5
Higgs yield	2.6 ± 0.5	0.72 ± 0.17	1.17 ± 0.25	11.2 ± 2.0	5.3 ± 1.0	5.5 ± 1.1
Other yield	2.1 ± 0.5	0.25 ± 0.17	0.39 ± 0.16	7.9 ± 1.5	4.0 ± 0.8	3.5 ± 0.8
Fake yield	1.3 ± 0.8	3.0 ± 1.5	$0.5^{+0.6}_{-0.5}$	6.4 ± 2.5	2.1 ± 1.1	3.6 ± 1.7

Region	$SR3\ell$	$SR3\ell_e$	$SR3\ell_\mu$
Observed yield	61	28	33
Expected background yield	54.9 ± 3.3	27.5 ± 2.2	27.4 ± 2.0
WZ yield	33.6 ± 2.4	16.5 ± 1.7	17.3 ± 1.8
ZZ yield	0.92 ± 0.27	0.11 ± 0.04	0.77 ± 0.24
$t\bar{t}Z$ yield	7.5 ± 2.3	4.1 ± 1.3	3.4 ± 0.7
Triboson yield	5.6 ± 1.5	2.7 ± 0.8	2.6 ± 0.7
Higgs yield	0.51 ± 0.10	0.25 ± 0.06	0.23 ± 0.05
Other yield	4.2 ± 0.8	2.0 ± 0.4	2.0 ± 0.4
Fake yield	2.5 ± 1.2	1.8 ± 1.1	1.0 ± 0.8

Model Independent Results

TABLE IV. Model-independent results where each row targets one $m_{Z\ell}$ bin of one SR and probes scenarios where a generic beyond-the-SM process is assumed to contribute only to that $m_{Z\ell}$ bin. The first two columns refer to the signal region and $m_{Z\ell}$ bin probed, while the third and fourth columns show the observed (N_{obs}) and expected (N_{exp}) event yields. The expected yields are obtained using a background-only fit of all the CRs, and the errors include statistical and systematic uncertainties. The fifth and sixth columns show the observed 95% C.L. upper limit on the visible cross section ($\langle\epsilon\sigma\rangle^{95}_{\text{obs}}$) and on the number of signal events (S^{95}_{obs}), while the seventh column shows the expected 95% C.L. upper limit on the number of signal events (S^{95}_{exp}) with the associated 1σ uncertainties. The last column provides the discovery p value and significance (Z) of any excess of data above background expectation. Cases for which the observed yield is less than the expected yield are capped at a p value of 0.5.

Region	Range of $m_{Z\ell}$ [GeV]	N_{obs}	N_{exp}	$\langle\epsilon\sigma\rangle^{95}_{\text{obs}}$ [fb]	S^{95}_{obs}	S^{95}_{exp}	$p(s=0)$ (Z)
SRFR	[90, 110]	2	1.58 ± 0.32	0.03	4.2	$4.0^{+1.8}_{-0.8}$	0.44 (0.2)
	[110, 130]	5	5.9 ± 1.0	0.04	5.6	$6.7^{+2.3}_{-2.1}$	0.50 (0.0)
	[130, 150]	2	6.0 ± 1.0	0.03	3.8	$6.3^{+2.0}_{-2.0}$	0.50 (0.0)
	[150, 170]	12	6.1 ± 1.0	0.10	14.3	$7.8^{+3.1}_{-1.9}$	0.02 (2.1)
	[170, 190]	5	4.5 ± 0.8	0.05	6.8	$5.8^{+2.2}_{-1.3}$	0.31 (0.5)
	[190, 210]	4	3.4 ± 0.6	0.04	6.2	$5.3^{+2.1}_{-1.2}$	0.28 (0.6)
	[210, 230]	2	2.6 ± 1.5	0.03	4.5	$4.8^{+1.9}_{-0.9}$	0.50 (0.0)
	[230, 250]	2	1.83 ± 0.31	0.03	4.7	$4.1^{+1.6}_{-0.8}$	0.41 (0.2)
	[250, 270]	1	1.25 ± 0.22	0.03	4.0	$3.9^{+1.2}_{-0.9}$	0.50 (0.0)
	[270, 300]	0	1.18 ± 0.32	0.03	3.6	$3.9^{+1.3}_{-0.8}$	0.50 (0.0)
	[300, 330]	3	0.89 ± 0.16	0.05	6.7	$4.2^{+0.8}_{-0.4}$	0.02 (2.0)
	[330, 360]	2	0.52 ± 0.18	0.04	5.6	$3.5^{+0.8}_{-0.2}$	0.03 (1.9)
	[360, 400]	1	0.50 ± 0.19	0.03	4.0	$3.2^{+1.0}_{-0.1}$	0.18 (0.9)
	[400, 440]	0	0.27 ± 0.09	0.02	3.2	$3.1^{+0.8}_{-0.1}$	0.50 (0.0)
	[440, 580]	1	0.29 ± 0.17	0.03	4.4	$3.3^{+1.0}_{-0.1}$	0.12 (1.2)
	> 580	0	$0.07^{+0.17}_{-0.07}$	0.02	3.0	$3.1^{+0.1}_{-0.0}$	0.50 (0.0)
SR4ℓ	[90, 110]	9	6.1 ± 0.7	0.07	9.6	$7.1^{+2.1}_{-1.1}$	0.14 (1.1)
	[110, 130]	22	15.4 ± 1.3	0.12	16.7	$10.0^{+4.4}_{-1.9}$	0.05 (1.6)
	[130, 150]	15	10.9 ± 0.9	0.09	12.8	$8.4^{+3.4}_{-1.8}$	0.09 (1.4)
	[150, 170]	10	7.9 ± 0.8	0.07	10.0	$7.5^{+2.9}_{-1.5}$	0.16 (1.0)
	[170, 190]	12	5.9 ± 0.6	0.10	14.2	$8.5^{+3.4}_{-0.8}$	0.02 (2.0)
	[190, 210]	7	4.9 ± 0.7	0.06	8.3	$6.5^{+1.9}_{-1.5}$	0.15 (1.0)
	[210, 230]	2	3.17 ± 0.33	0.03	4.4	$4.9^{+2.2}_{-1.4}$	0.50 (0.0)
	[230, 250]	2	2.36 ± 0.27	0.03	4.5	$4.5^{+1.9}_{-1.1}$	0.50 (0.0)
	[250, 270]	2	2.1 ± 0.5	0.03	4.9	$4.8^{+1.8}_{-1.2}$	0.50 (0.0)
	[270, 300]	2	1.88 ± 0.21	0.03	4.8	$4.2^{+1.6}_{-1.0}$	0.50 (0.0)
	[300, 330]	1	1.03 ± 0.14	0.03	4.1	$3.6^{+1.6}_{-0.5}$	0.50 (0.0)
	[330, 360]	1	0.88 ± 0.21	0.03	4.0	$3.7^{+1.4}_{-0.7}$	0.26 (0.6)
	[360, 400]	0	0.84 ± 0.20	0.02	3.0	$3.4^{+1.5}_{-0.4}$	0.50 (0.0)
	[400, 440]	1	0.64 ± 0.18	0.03	4.2	$3.2^{+1.1}_{-0.1}$	0.17 (1.0)
	[440, 580]	2	2.0 ± 0.4	0.03	4.7	$4.6^{+1.5}_{-1.1}$	0.50 (0.0)
	> 580	1	2.3 ± 0.4	0.03	4.0	$4.7^{+1.7}_{-0.8}$	0.50 (0.0)

TABLE IV. *(Continued)*

Region	Range of $m_{Z\ell}$ [GeV]	N_{obs}	N_{exp}	$\langle\epsilon\sigma\rangle^{95}_{\text{obs}}$ [fb]	S^{95}_{obs}	S^{95}_{exp}	$p(s=0)$ (Z)
SR3ℓ	[90, 110]	0	1.08 ± 0.18	0.03	4.8	$3.8^{+1.3}_{-0.5}$	0.50 (0.0)
	[110, 130]	5	2.8 ± 0.4	0.06	7.9	$5.6^{+1.7}_{-0.9}$	0.08 (1.4)
	[130, 150]	5	4.1 ± 0.6	0.05	6.7	$5.8^{+2.0}_{-1.2}$	0.26 (0.6)
	[150, 170]	2	4.0 ± 0.6	0.03	4.1	$5.3^{+2.3}_{-1.2}$	0.50 (0.0)
	[170, 190]	3	3.9 ± 0.4	0.03	4.9	$5.2^{+2.4}_{-1.1}$	0.50 (0.0)
	[190, 210]	7	3.7 ± 0.6	0.07	9.1	$6.1^{+2.2}_{-1.9}$	0.10 (1.3)
	[210, 230]	6	3.5 ± 0.7	0.06	8.8	$6.2^{+1.8}_{-1.7}$	0.08 (1.4)
	[230, 250]	4	3.3 ± 0.6	0.04	6.1	$5.3^{+1.7}_{-1.2}$	0.28 (0.6)
	[250, 270]	3	2.5 ± 0.4	0.04	5.1	$4.5^{+1.8}_{-1.3}$	0.36 (0.4)
	[270, 300]	3	3.7 ± 0.4	0.03	4.8	$5.4^{+1.8}_{-1.6}$	0.50 (0.0)
	[300, 330]	3	3.0 ± 0.4	0.04	5.1	$4.9^{+1.8}_{-1.1}$	0.50 (0.0)
	[330, 360]	2	2.06 ± 0.35	0.03	4.8	$4.5^{+1.5}_{-1.4}$	0.50 (0.0)
	[360, 400]	3	3.2 ± 0.7	0.04	5.1	$5.3^{+2.0}_{-1.5}$	0.50 (0.0)
	[400, 440]	0	1.70 ± 0.27	0.02	3.0	$3.7^{+2.0}_{-0.6}$	0.50 (0.0)
	[440, 580]	7	4.3 ± 0.5	0.06	8.7	$6.2^{+1.9}_{-1.3}$	0.09 (1.3)
	> 580	8	4.6 ± 0.6	0.07	10.0	$6.5^{+2.3}_{-1.4}$	0.08 (1.4)

Setting Limits: Model Independent

- Model independent limits are derived at 95% confidence level (C.L.) using the CLs prescription, and results are evaluated using pseudoexperiments.

- A profile likelihood fit is performed on the numbers of observed and expected events in the target $m_{Z\ell}$ bin of one SR and the three CRs, and a generic BSM process is assumed to contribute only to the target $m_{Z\ell}$ bin

- In this way no assumption is made concerning the $\chi_1^{\pm}/\chi_1^0$ branching fractions or mZl shape of the BSM process

Setting Limits: Model Independent

TABLE IV. Model-independent results where each row targets one $m_{Z\ell}$ bin of one SR and probes scenarios where a generic beyond-the-SM process is assumed to contribute only to that $m_{Z\ell}$ bin. The first two columns refer to the signal region and $m_{Z\ell}$ bin probed, while the third and fourth columns show the observed (N_{obs}) and expected (N_{exp}) event yields. The expected yields are obtained using a background-only fit of all the CRs, and the errors include statistical and systematic uncertainties. The fifth and sixth columns show the observed 95% C.L. upper limit on the visible cross section ($\langle\epsilon\sigma\rangle^{95}_{\text{obs}}$) and on the number of signal events (S^{95}_{obs}), while the seventh column shows the expected 95% C.L. upper limit on the number of signal events (S^{95}_{exp}) with the associated 1σ uncertainties. The last column provides the discovery p value and significance (Z) of any excess of data above background expectation. Cases for which the observed yield is less than the expected yield are capped at a p value of 0.5.

Region	Range of $m_{Z\ell}$ [GeV]	N_{obs}	N_{exp}	$\langle\epsilon\sigma\rangle^{95}_{\text{obs}}$ [fb]	S^{95}_{obs}	S^{95}_{exp}	$p(s=0)$ (Z)
SRFR	[90, 110]	2	1.58 ± 0.32	0.03	4.2	$4.0^{+1.8}_{-0.8}$	0.44 (0.2)
	[110, 130]	5	5.9 ± 1.0	0.04	5.6	$6.7^{+2.3}_{-2.1}$	0.50 (0.0)
	[130, 150]	2	6.0 ± 1.0	0.03	3.8	$6.3^{+2.0}_{-2.0}$	0.50 (0.0)
	[150, 170]	12	6.1 ± 1.0	0.10	14.3	$7.8^{+3.1}_{-1.9}$	0.02 (2.1)
	[170, 190]	5	4.5 ± 0.8	0.05	6.8	$5.8^{+2.2}_{-1.3}$	0.31 (0.5)
	[190, 210]	4	3.4 ± 0.6	0.04	6.2	$5.3^{+2.1}_{-1.2}$	0.28 (0.6)
	[210, 230]	2	2.6 ± 1.5	0.03	4.5	$4.8^{+1.9}_{-0.9}$	0.50 (0.0)
	[230, 250]	2	1.83 ± 0.31	0.03	4.7	$4.1^{+1.6}_{-0.8}$	0.41 (0.2)
	[250, 270]	1	1.25 ± 0.22	0.03	4.0	$3.9^{+1.2}_{-0.9}$	0.50 (0.0)
	[270, 300]	0	1.18 ± 0.32	0.03	3.6	$3.9^{+1.3}_{-0.8}$	0.50 (0.0)
	[300, 330]	3	0.89 ± 0.16	0.05	6.7	$4.2^{+0.8}_{-0.4}$	0.02 (2.0)
	[330, 360]	2	0.52 ± 0.18	0.04	5.6	$3.5^{+0.8}_{-0.2}$	0.03 (1.9)
	[360, 400]	1	0.50 ± 0.19	0.03	4.0	$3.2^{+1.0}_{-0.1}$	0.18 (0.9)
	[400, 440]	0	0.27 ± 0.09	0.02	3.2	$3.1^{+0.8}_{-0.1}$	0.50 (0.0)
	[440, 580]	1	0.29 ± 0.17	0.03	4.4	$3.3^{+1.0}_{-0.1}$	0.12 (1.2)
	> 580	0	$0.07^{+0.17}_{-0.07}$	0.02	3.0	$3.1^{+0.1}_{-0.0}$	0.50 (0.0)
SR4ℓ	[90, 110]	9	6.1 ± 0.7	0.07	9.6	$7.1^{+2.1}_{-1.1}$	0.14 (1.1)
	[110, 130]	22	15.4 ± 1.3	0.12	16.7	$10.0^{+4.4}_{-1.9}$	0.05 (1.6)
	[130, 150]	15	10.9 ± 0.9	0.09	12.8	$8.4^{+3.4}_{-1.8}$	0.09 (1.4)
	[150, 170]	10	7.9 ± 0.8	0.07	10.0	$7.5^{+2.9}_{-1.5}$	0.16 (1.0)
	[170, 190]	12	5.9 ± 0.6	0.10	14.2	$8.5^{+3.4}_{-0.8}$	0.02 (2.0)
	[190, 210]	7	4.9 ± 0.7	0.06	8.3	$6.5^{+1.9}_{-1.5}$	0.15 (1.0)
	[210, 230]	2	3.17 ± 0.33	0.03	4.4	$4.9^{+2.2}_{-1.4}$	0.50 (0.0)
	[230, 250]	2	2.36 ± 0.27	0.03	4.5	$4.5^{+1.9}_{-1.1}$	0.50 (0.0)
	[250, 270]	2	2.1 ± 0.5	0.03	4.9	$4.8^{+1.8}_{-1.2}$	0.50 (0.0)
	[270, 300]	2	1.88 ± 0.21	0.03	4.8	$4.2^{+1.6}_{-1.0}$	0.50 (0.0)
	[300, 330]	1	1.03 ± 0.14	0.03	4.1	$3.6^{+1.6}_{-0.5}$	0.50 (0.0)
	[330, 360]	1	0.88 ± 0.21	0.03	4.0	$3.7^{+1.4}_{-0.7}$	0.26 (0.6)
	[360, 400]	0	0.84 ± 0.20	0.02	3.0	$3.4^{+1.5}_{-0.4}$	0.50 (0.0)
	[400, 440]	1	0.64 ± 0.18	0.03	4.2	$3.2^{+1.1}_{-0.1}$	0.17 (1.0)
	[440, 580]	2	2.0 ± 0.4	0.03	4.7	$4.6^{+1.5}_{-1.1}$	0.50 (0.0)
	> 580	1	2.3 ± 0.4	0.03	4.0	$4.7^{+1.7}_{-0.8}$	0.50 (0.0)

TABLE IV. *(Continued)*

Region	Range of $m_{Z\ell}$ [GeV]	N_{obs}	N_{exp}	$\langle\epsilon\sigma\rangle^{95}_{\text{obs}}$ [fb]	S^{95}_{obs}	S^{95}_{exp}	$p(s=0)$ (Z)
SR3ℓ	[90, 110]	0	1.08 ± 0.18	0.03	4.8	$3.8^{+1.3}_{-0.5}$	0.50 (0.0)
	[110, 130]	5	2.8 ± 0.4	0.06	7.9	$5.6^{+1.7}_{-0.9}$	0.08 (1.4)
	[130, 150]	5	4.1 ± 0.6	0.05	6.7	$5.8^{+2.0}_{-1.2}$	0.26 (0.6)
	[150, 170]	2	4.0 ± 0.6	0.03	4.1	$5.3^{+2.3}_{-1.2}$	0.50 (0.0)
	[170, 190]	3	3.9 ± 0.4	0.03	4.9	$5.2^{+2.4}_{-1.1}$	0.50 (0.0)
	[190, 210]	7	3.7 ± 0.6	0.07	9.1	$6.1^{+2.2}_{-1.9}$	0.10 (1.3)
	[210, 230]	6	3.5 ± 0.7	0.06	8.8	$6.2^{+1.8}_{-1.7}$	0.08 (1.4)
	[230, 250]	4	3.3 ± 0.6	0.04	6.1	$5.3^{+1.7}_{-1.2}$	0.28 (0.6)
	[250, 270]	3	2.5 ± 0.4	0.04	5.1	$4.5^{+1.8}_{-1.3}$	0.36 (0.4)
	[270, 300]	3	3.7 ± 0.4	0.03	4.8	$5.4^{+1.8}_{-1.6}$	0.50 (0.0)
	[300, 330]	3	3.0 ± 0.4	0.04	5.1	$4.9^{+1.8}_{-1.1}$	0.50 (0.0)
	[330, 360]	2	2.06 ± 0.35	0.03	4.8	$4.5^{+1.5}_{-1.4}$	0.50 (0.0)
	[360, 400]	3	3.2 ± 0.7	0.04	5.1	$5.3^{+2.0}_{-1.5}$	0.50 (0.0)
	[400, 440]	0	1.70 ± 0.27	0.02	3.0	$3.7^{+2.0}_{-0.6}$	0.50 (0.0)
	[440, 580]	7	4.3 ± 0.5	0.06	8.7	$6.2^{+1.9}_{-1.3}$	0.09 (1.3)
	> 580	8	4.6 ± 0.6	0.07	10.0	$6.5^{+2.3}_{-1.4}$	0.08 (1.4)

Distributions of the data and postfit background in the CRs and VRs that are relevant in the extrapolation to the SRs

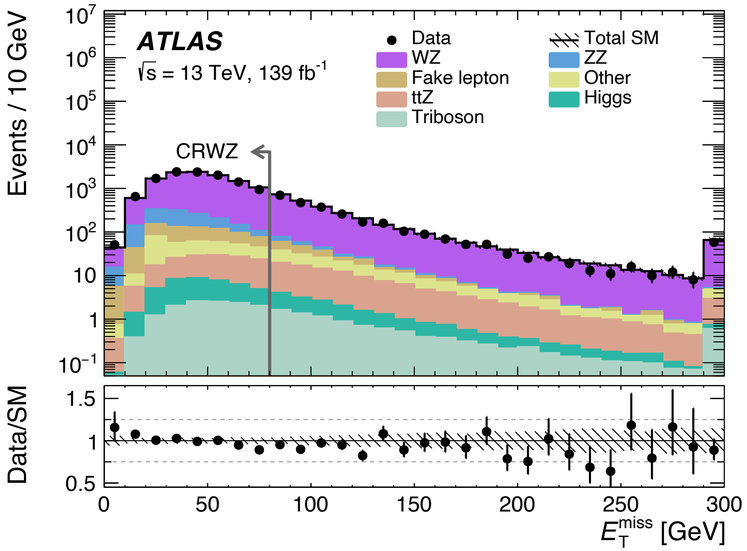

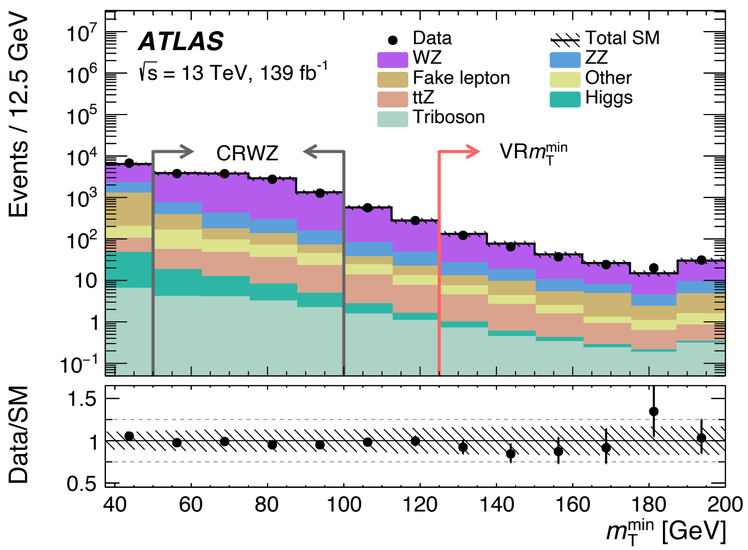

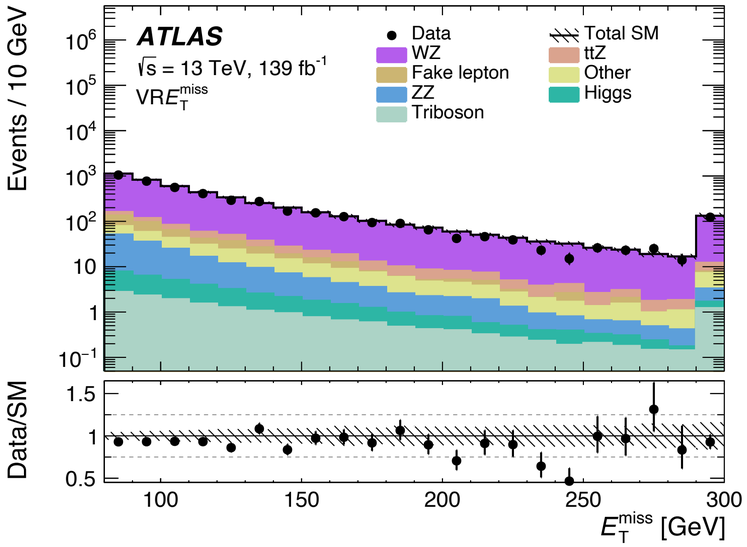

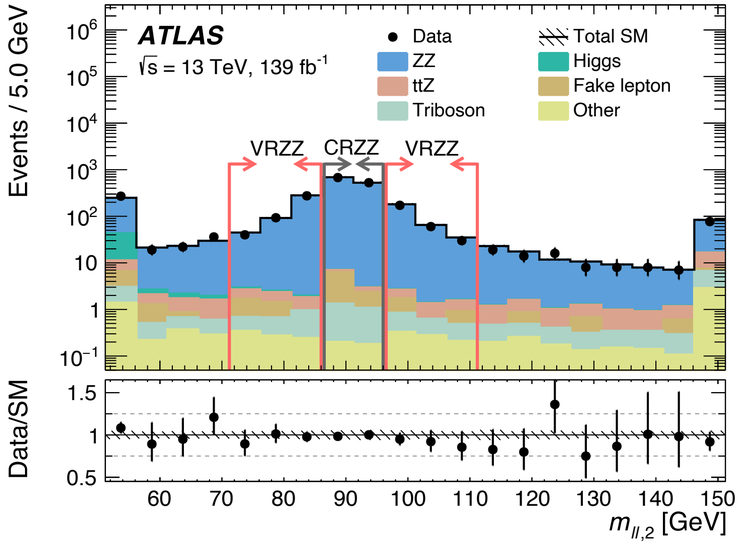

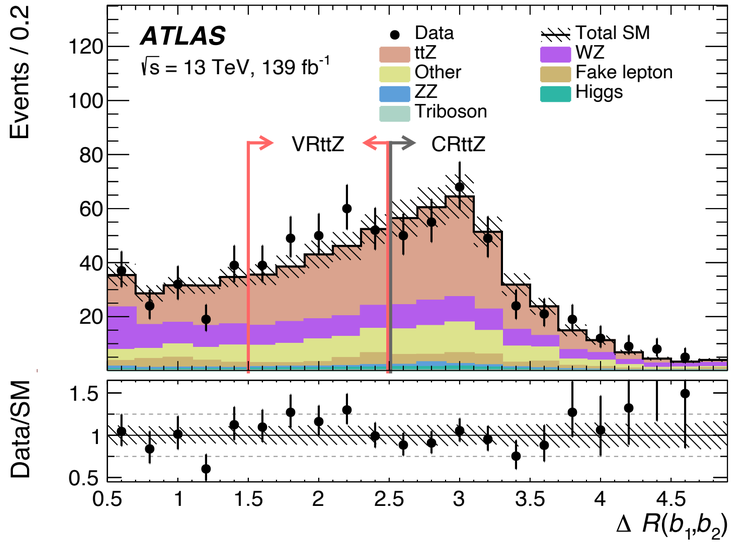

The mZl distributions of the data and postfit background in the CR and VRs

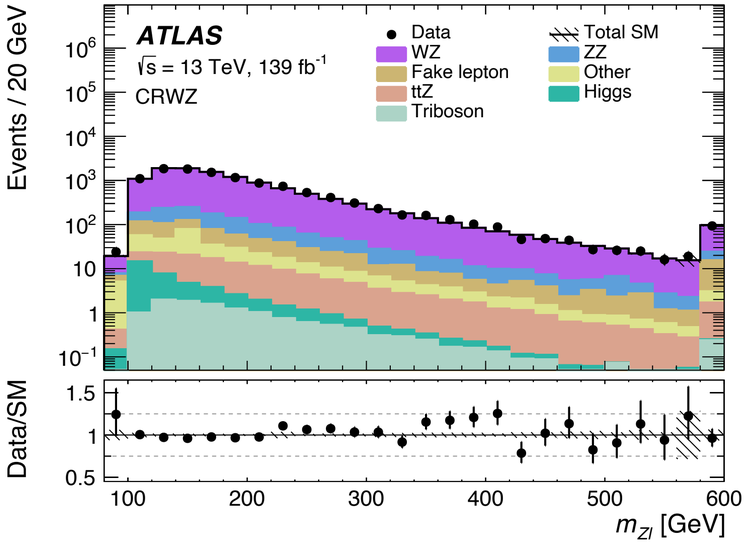

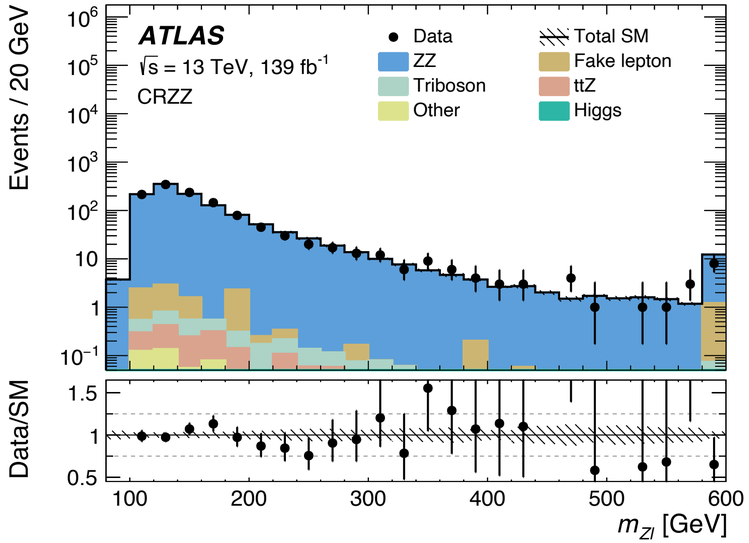

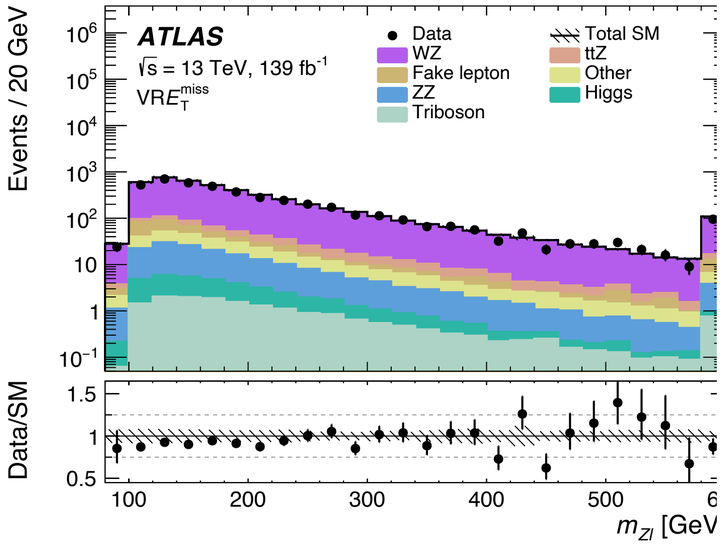

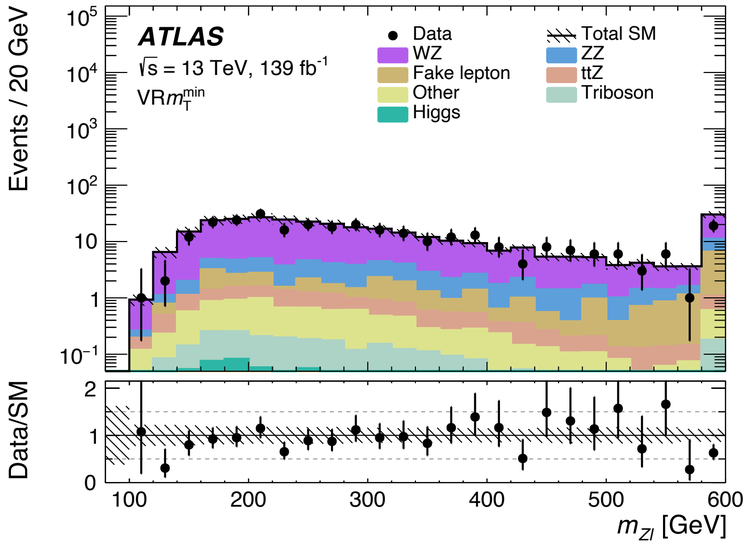

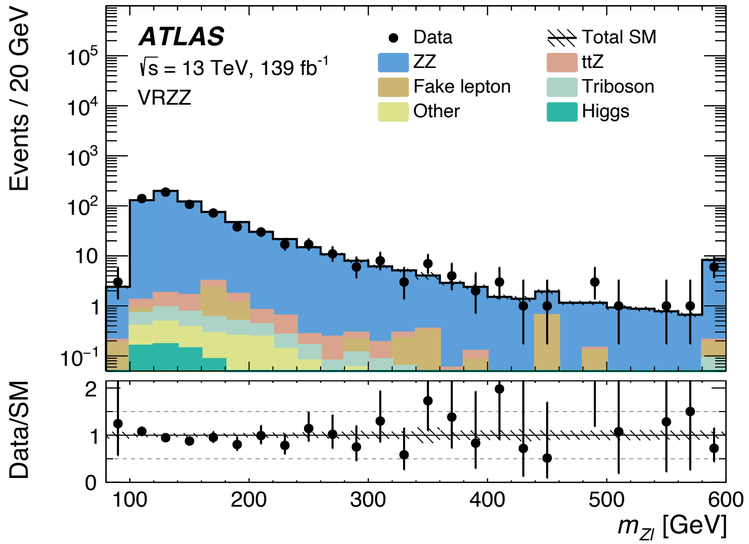

The mZl distributions of the data and postfit background in the CR and VRs

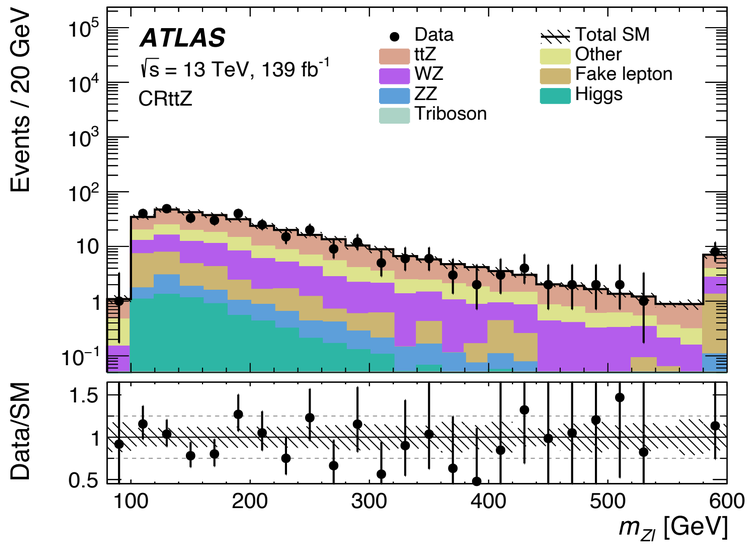

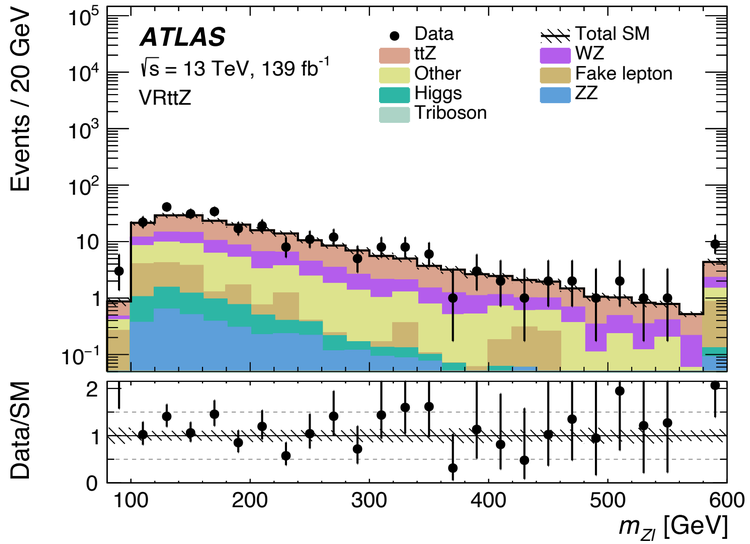

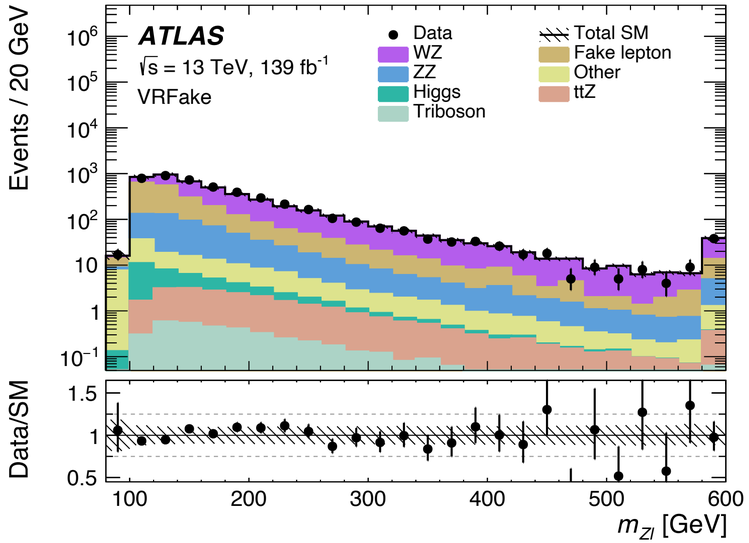

The relative uncertainties in the postfit SM background prediction as a function of mZl from the background-only fit

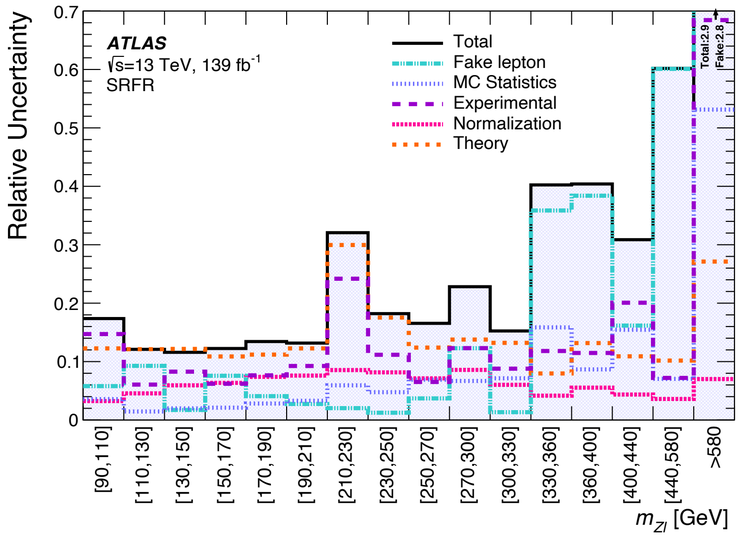

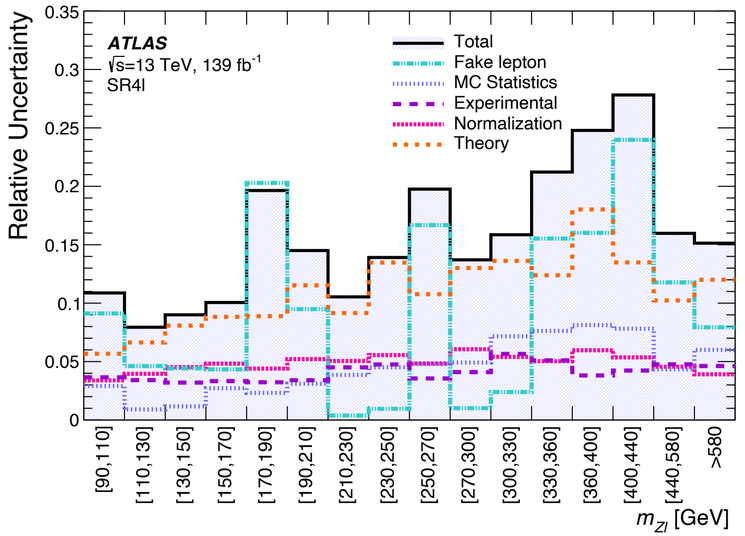

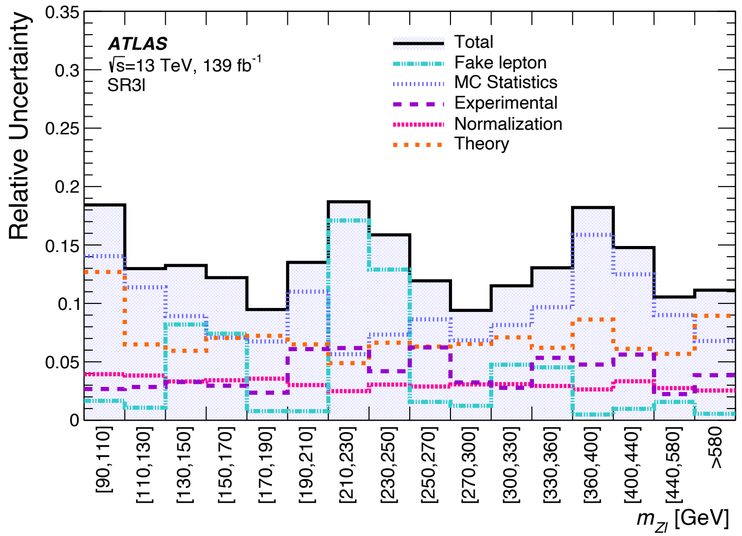

Object Selection

Baseline objects

Baseline muons:
- $|\eta|<2.7$, $p_T>10$ GeV,
- $z_0 \sin\theta<0.5$,
- ID: Medium

Baseline electrons:
- $|\eta|<2.47$, $p_T>10$ GeV,
- $z_0 \sin\theta<0.5$,
- Crack veto, Quality cuts,
- ID: LooseAndBLayerLLH

Baseline jets:
- $p_T>20$ GeV
- AntiKt4EMTopo, R=0.4

Overlap removal: HF-aware for b-jet
$p_T< 100$ GeV (MV2c10, Fixed 85%)

MET: Tight WP, using electrons, muons, jets, and photons

Signal objects

Signal muons:
- $p_T>12$ GeV,
- Iso: FCTight_FixedRad,
- $-d_0/\sigma(d_0)<3$,
- cosmic veto,
- bad muon event veto

Signal electrons:
- $p_T>12$ GeV,
- ID: MediumLLH,
- Iso: FCTight,
- $d_0/\sigma(d_0)<5$

Signal jets:
$|\eta|<2.8$,
- Medium JVT for $p_T<120$ GeV and $|\eta|<2.5$,
- bad jet event veto

b jets:
- $|\eta|<2.5$, MV2c10, Fixed 85%

- **Preselection:** Require at least 3 signal leptons, 2 of which are SFOS within [81,101] GeV. Using **SUSY2** derivations and requiring that a **single lepton trigger** is fired by a signal lepton.

Region Definitions: SROL3ℓ

Region	N_{lep}	$N_{\text{b-jet}}$	$\Delta R(b,b)$†	$E_{\text{T}}^{\text{miss}}$ [GeV]	$m_{\text{T}}^{\text{min}}$ [GeV]	Second boson	$4\ell 2Z$; $\lvert m_{\ell\ell,2} - m_Z \rvert$ [GeV]	$m_{Z\ell}$ asymmetry
SROL3ℓ	==3	-	<1.5	>150	>125	-	-	-
CRWZ	==3	-	<1.5	<80	[50,100]	-	-	-
VRMet	==3	-	<1.5	>80	<100	-	-	-
VRmTmin	==3	-	<1.5	<80	>125	-	-	-
CRZj	==3	-	<1.5	<30	<30	-	-	-
VRZj	==3	-	<1.5	[30,80]	<30	-	-	-
CRttZ	≥3	≥2	>2.5	>40	-	-	veto; <20	-
VRttZ	≥3	≥2	[1.5,2.5]	>40	-	-	veto; <20	-
SROL4ℓ	≥4	-	<1.5	>80*	-	No	veto; <20	-
SRTL	≥4	-	<1.5	-	-	Yes	veto; <20	< 0.1
CRZZ	==4	-	<1.5	-	-	-	require; <5	-
VRZZ	==4	-	<1.5	-	-	-	require; [5,20]	-

- $\Delta R(b_0,b_1)$: The angular separation between the two hardest b-jets in an event, (†) indicates that this cut is only applied for events with at least 2 b-jets
- E_T^{miss}: *missing transverse energy, expect real met in these events*
- m_T^{min}: *min of* $m_T^2(\ell,\nu) = 2p_T^{\ell}E_T^{miss}[1-\cos(\phi_{\ell}-\phi_{miss})]$

Region Definitions: SROL4ℓ

Region	N_{lep}	$N_{\text{b-jet}}$	$\Delta R(b,b)$†	$E_{\text{T}}^{\text{miss}}$ [GeV]	$m_{\text{T}}^{\text{min}}$ [GeV]	Second boson	$4\ell 2Z$; $\lvert m_{\ell\ell,2} - m_Z \rvert$ [GeV]	$m_{Z\ell}$ asymmetry
SROL3ℓ	==3	-	<1.5	>150	>125	-	-	-
CRWZ	==3	-	<1.5	<80	[50,100]	-	-	-
VRMet	==3	-	<1.5	>80	<100	-	-	-
VRmTmin	==3	-	<1.5	<80	>125	-	-	-
CRZj	==3	-	<1.5	<30	<30	-	-	-
VRZj	==3	-	<1.5	[30,80]	<30	-	-	-
CRttZ	≥3	≥2	>2.5	>40	-	-	veto; <20	-
VRttZ	≥3	≥2	[1.5,2.5]	>40	-	-	veto; <20	-
SROL4ℓ	≥4	-	<1.5	>80*	-	No	veto; <20	-
SRTL	≥4	-	<1.5	-	-	Yes	veto; <20	< 0.1
CRZZ	==4	-	<1.5	-	-	-	require; <5	-
VRZZ	==4	-	<1.5	-	-	-	require; [5,20]	-

- E_T^{miss} : (*) indicates that this cut is only applied for events with two pairs of SF leptons,⇒ $E_T^{miss} \rightarrow E_T^{miss,SF}$
- 4l2Z: True for events with exactly 4 leptons and 2 pairs of SFOS leptons,
  - One SFOS pair, $m_{\ell\ell}$, required $(m_Z\text{-}10) < m_{\ell\ell} < (m_Z+10)$, as per Presel.
  - Mass requirement on the second SFOS pair, $m_{\ell\ell,2}$, varies for each region

Region Definitions: SRTL

Region	N_{lep}	$N_{\text{b-jet}}$	$\Delta R(b,b)$†	$E_{\text{T}}^{\text{miss}}$ [GeV]	$m_{\text{T}}^{\text{min}}$ [GeV]	Second boson	$4\ell 2Z$; $\lvert m_{\ell\ell,2} - m_Z \rvert$ [GeV]	$m_{Z\ell}$ asymmetry
SROL3ℓ	==3	-	<1.5	>150	>125	-	-	-
CRWZ	==3	-	<1.5	<80	[50,100]	-	-	-
VRMet	==3	-	<1.5	>80	<100	-	-	-
VRmTmin	==3	-	<1.5	<80	>125	-	-	-
CRZj	==3	-	<1.5	<30	<30	-	-	-
VRZj	==3	-	<1.5	[30,80]	<30	-	-	-
CRttZ	≥3	≥2	>2.5	>40	-	-	veto; <20	-
VRttZ	≥3	≥2	[1.5,2.5]	>40	-	-	veto; <20	-
SROL4ℓ	≥4	-	<1.5	>80*	-	No	veto; <20	-
SRTL	≥4	-	<1.5	-	-	Yes	veto; <20	< 0.1
CRZZ	==4	-	<1.5	-	-	-	require; <5	-
VRZZ	==4	-	<1.5	-	-	-	require; [5,20]	-

$$m_{Z\ell}^{\text{asym}} = \frac{|m_{Z\ell} - m_{B\ell}|}{(m_{Z\ell} + m_{B\ell})}$$

: Asymmetry should be small if the boson-lepton pairs come from a particle with the same mass

Fake Lepton Background Estimation

fake process	CRWZ	VRMet	VRmTmin	CRttZ	VRttZ	SROL3l	SROL4l	SRTL
Z+jets/$Z+\gamma$	74%	47%	63%	37%	23%	41%	22%	5%
WZ	-	-	-	-	-	-	45%	21%
ZZ	-	-	-	-	-	-	15%	19%
ttV	-	-	-	-	-	-	-	40%
top-like	20%	43%	28%	54%	69%	48%	3%	10%
tot. fake / tot. bkgd	4%	5%	8%	12%	11%	7%	5%	2%

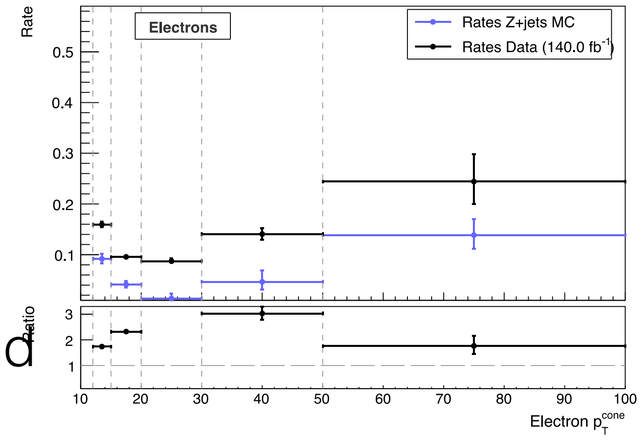

- Relative contributions of each process to the fake and total background in various analysis regions
- Fake background small in signal regions (7% or less)
- Fake Factor method used to estimate the fake background
- Derive the FFs in a region dominated by Z+jets events with fake leptons
- Apply these Z+jets FFs to anti-ID events from all processes
- Parameterized in p_T^{cone}= p_T + iso cone instead of p_T
  - Better handle on underlying jet
  - Less process dependence. Z+jets HF fakes ~ ttbar HF fakes
  - Gave best agreement in FF VR and other analysis regions

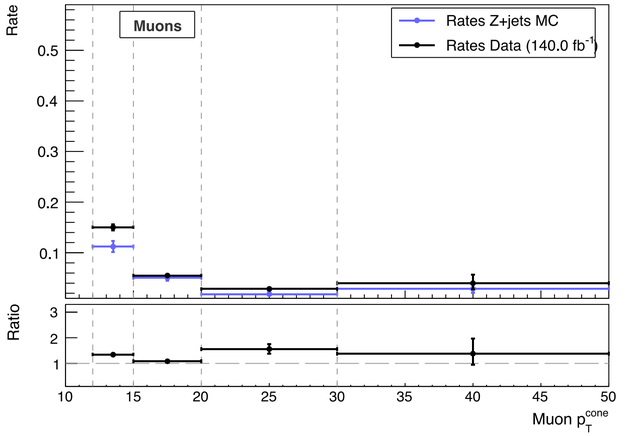

Object Selection

- 3 types of Signal regions (SRs) defined by way of the object selection
- **SR3ℓ**: 3 Leptons
- **SR4ℓ**: 4 Leptons
- **SRFR**: Fully Reconstructed

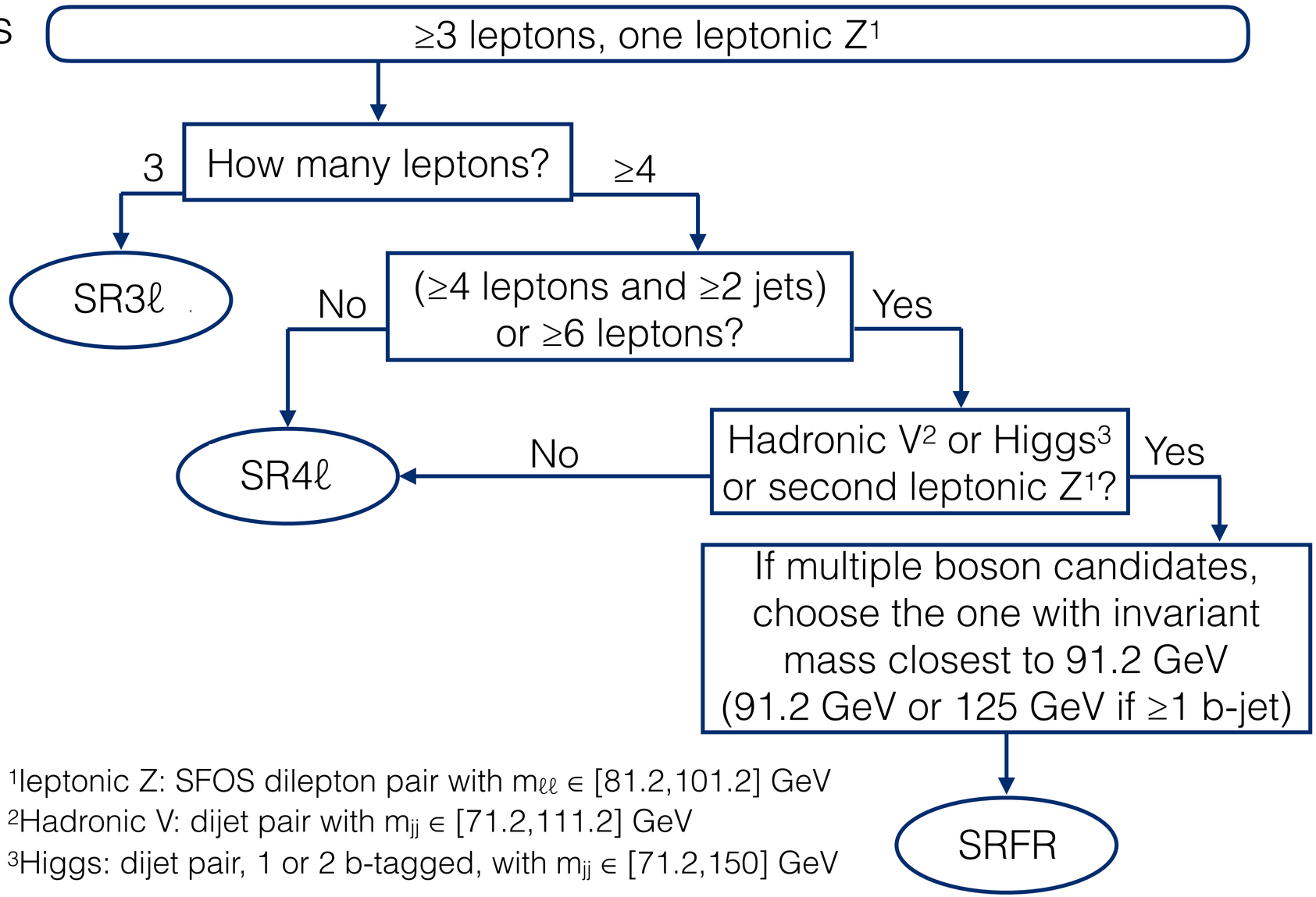

[1]leptonic Z: SFOS dilepton pair with $m_{\ell\ell} \in [81.2,101.2]$ GeV
[2]Hadronic V: dijet pair with $m_{jj} \in [71.2,111.2]$ GeV
[3]Higgs: dijet pair, 1 or 2 b-tagged, with $m_{jj} \in [71.2,150]$ GeV

Object Selection: Algorithms in Brief

- **SR3ℓ**: Very straight forward → just compute the invariant mass of the 3 leptons
- **SR4ℓ**: Very much not straight forward → If a 2nd boson **is not** reconstructed there is ambiguity as to which lepton should be used for the trilepton leg. Because of the varying kinematics depending on chargino mass, **there is no lepton matching choice that performs best for all mass points**. Many options were studied and the chosen scheme uses L_T, the scalar sum of the p_T of all leptons in an event, as a proxy for the chargino mass.
  - L_T <550 GeV: lepton closest in ΔR to the Z is assigned. At low mass the Z and the lepton from the same chargino leg are generally collimated
  - L_T >550 GeV: lepton which maximizes $m_{Z\ell}$ is assigned. At high mass it is unlikely that a random combination of $Z\ell$ pairs would have a large invariant mass, in both signal and background
- **SRFR**: Pretty straight forward → A 2nd boson (besides the Z) is successfully reconstructed and the leptons are matched in a way that the $m_{Z\ell}$ asymmetry = $|m_{Z\ell} - m_{B\ell}| / (m_{Z\ell}+m_{B\ell})$ is minimized

Limit Setting Strategy

- We will set limits across the full plane of possible wino decays by reweighting signal events according to truth decay
- Do a coarse scan in lepton flavor:
  - (BR($\chi^{\pm}_{W}\rightarrow$Be), BR($\chi^{\pm}_{W}\rightarrow$Bμ), BR($\chi^{\pm}_{W}\rightarrow$Bτ))=(1,0,0), (0,1,0), (0,0,1), (0.33,0.33,0.34)
  - For BR($\chi^{\pm}_{W}\rightarrow$Be/Bμ)=1, require that non-Z lepton is e or μ
    - SR3ℓ, SR4ℓ: requirement only on non-Z lepton
    - SRFR: requirement on both non-boson leptons
    - Effectively tripling our SR count. Expected yield tables will be included in appendix.
- For each of these lepton BR points, do a fine scan of boson BR (increments of 0.25 or smaller)
  - Each lepton BR point will have a corresponding triangle limit plot (Higgs BR vs Z BR)
- $\chi^{\pm}_{W}\,\chi^{0}_{W}$: Set BR($\chi^{\pm}_{W}\rightarrow$Zℓ)=1. Ignoring possible correlations between $\chi^{\pm}_{W}$ and χ^{0}_{W} BRs. No large correlation seen by theorists.

Uncertainties

- Detector uncertainties: CP/PMG/SUSY recommendations are used.
  - Jet energy scale and resolution (8 JES and 8 JER), flavor tagging, pileup tagging
  - Lepton scale and resolution and efficiencies (including trigger)
  - MET uncertainties
  - Luminosity: 1.7%
- Theory systematics:
  - Diboson, Triboson, and ttZ samples:
    - Using internal weights (scale, αS, PDF). Diboson and Triboson are ready, currently implemented in HF as a flat systematic. Results binned in mZℓ are available but not yet implemented in HF.
    - We will run available alternative samples through SimpleAnalysis for hard scatter, PS, ISR. Not all samples are available (ttZ ISR)
  - Other background samples, including Higgs: flat uncertainty is taken
  - Signal samples: Private alternative samples will be generated to assess relevant variations.
- Fake systematics:
  - Propagation of statistical uncertainty from measurement region
  - Prompt subtraction, to account for MC cross section uncertainty
  - Closure, to account for differences in source and composition between regions
  - Parameterization, to account for FF dependence on kinematic variables other than pTcone

Search Motivation: Signals of Interest

- Mass splitting between $\chi^{\pm}_{W}$ and χ^{0}_{W} is small regardless of which is LSP (≤200 MeV for most cases)
- Can assume **both particles RPV decay**

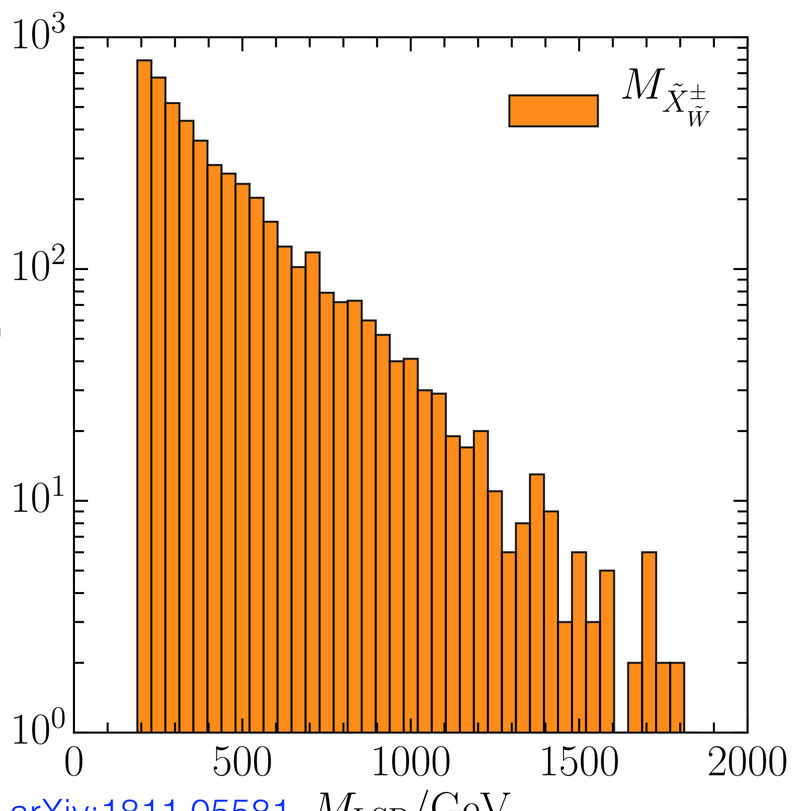

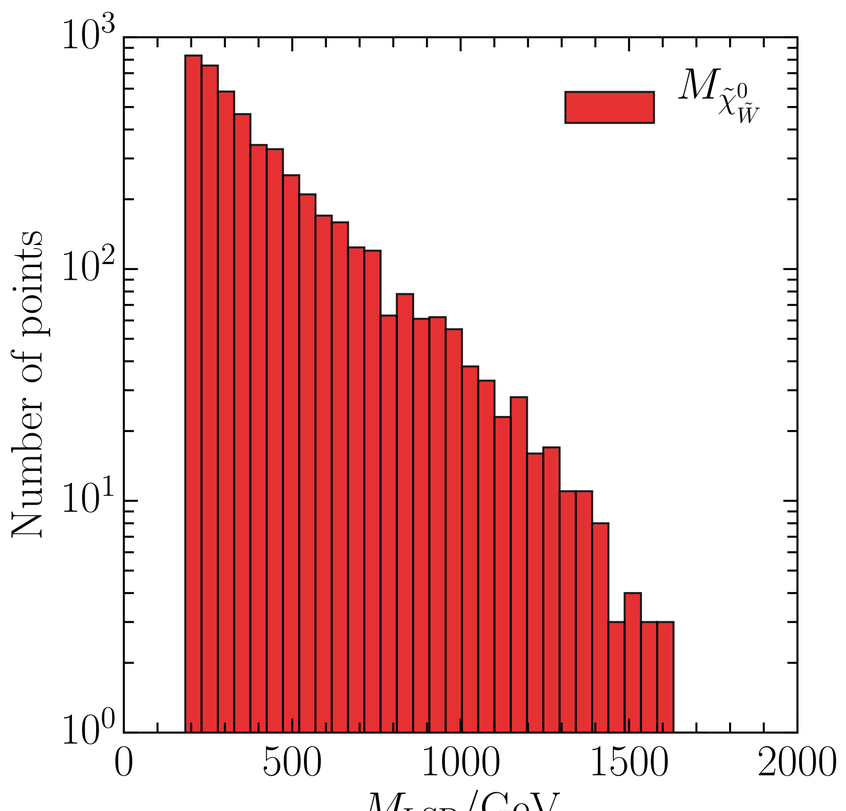

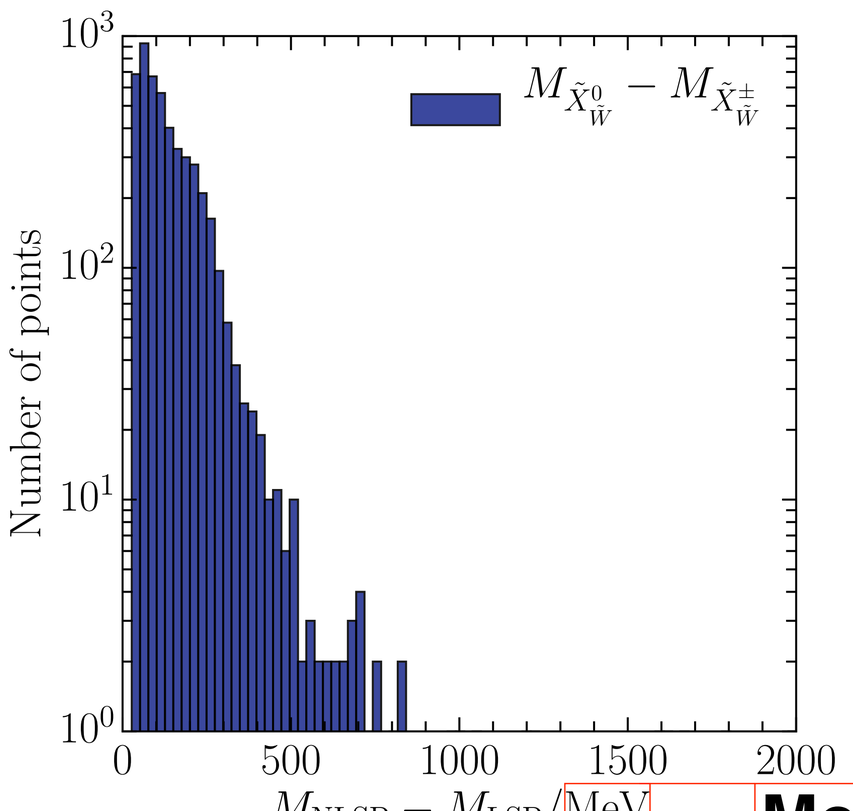

arXiv:1811.05581

Search Motivation: Signals of Interest

- Targeting the very visible 3-lepton resonance $\chi^{\pm}_{W} \rightarrow Z\ell^{\pm} \rightarrow \ell^{\pm}\ell^{\mp}\ell^{\pm}$
- The reconstruction of $\chi^{0}_{W} \rightarrow W\ell^{\pm} \rightarrow qq\ell^{\pm}$ and $\chi^{\pm}_{W} \rightarrow H\ell^{\pm} \rightarrow bb\ell^{\pm}$ when possible* also adds sensitivity
- We are setting limits for a large scan of $\chi^{\pm}_{W}$ and χ^{0}_{W} BRs which will cover the other possible decays

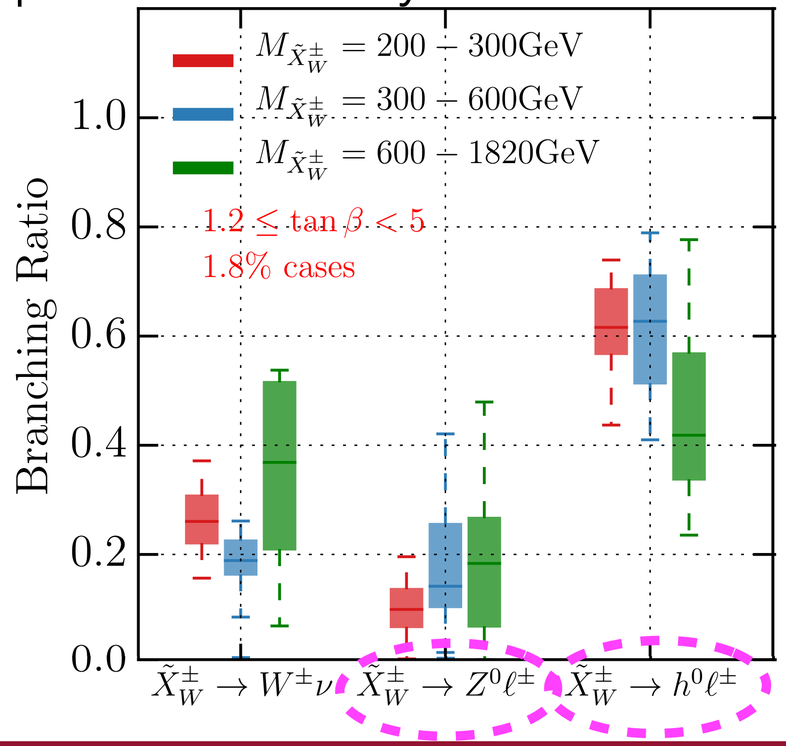

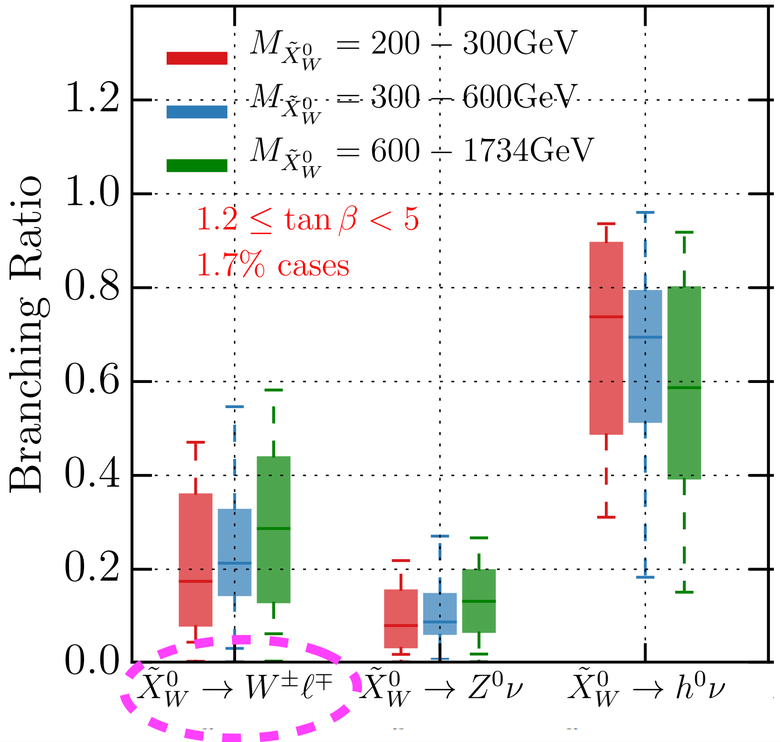

*discussed in “Two Leg” alg in slide 12

arXiv:1811.05581

Signals of Interest: $\chi^{\pm}_{W}$ and χ^{0}_{W} BRs

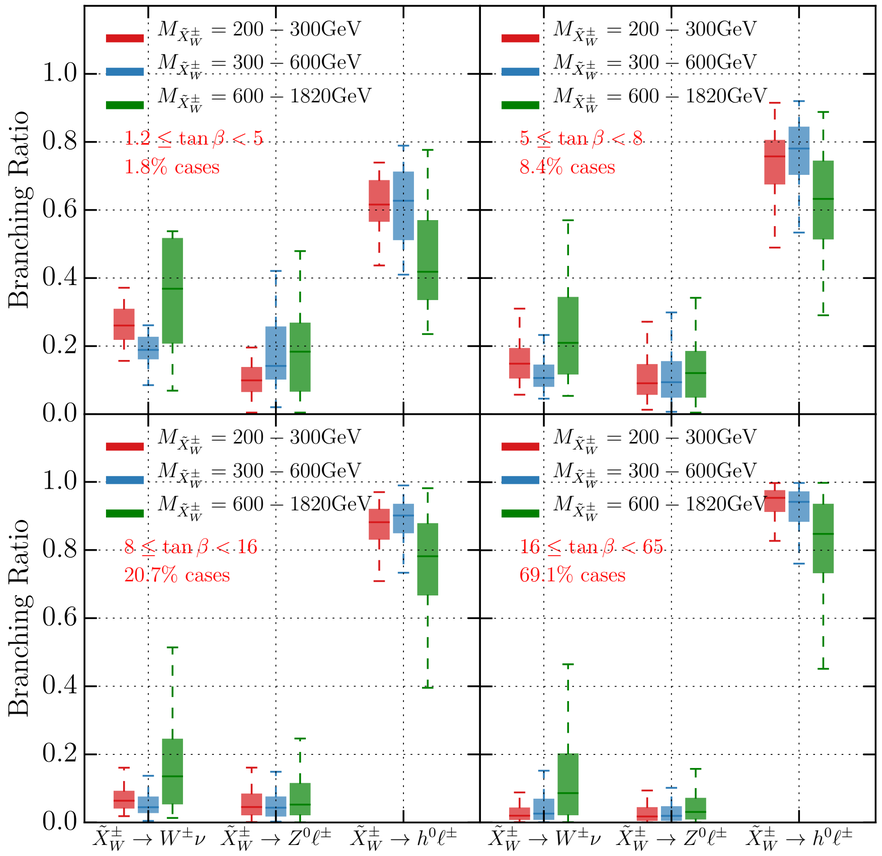

Figure 6: Branching ratios for the four possible decay channels of the Wino chargino LSP, presented for the three $M_{\tilde{X}^{\pm}_W}$ mass bins and four $\tan\beta$ regions. The colored horizontal line inside each box indicate the median value of the branching fraction in that bin, the colored box indicates the interquartile range in that bin, while the dashed error bars show the range between the maximum and the minimum values of the branching ratio for that bin. The case percentage indicate what percentage of the valid initial points have $\tan\beta$ values within the range indicated. For each channel, we sum over all three families of possible leptons. Note that $\tilde{X}^{\pm}_W \to h^0\ell^{\pm}$ is strongly favored– except perhaps in the $1.2 < \tan\beta < 5$ bin. The calculations were performed assuming a normal neutrino hierarchy, with $\theta_{23} = 0.597$.

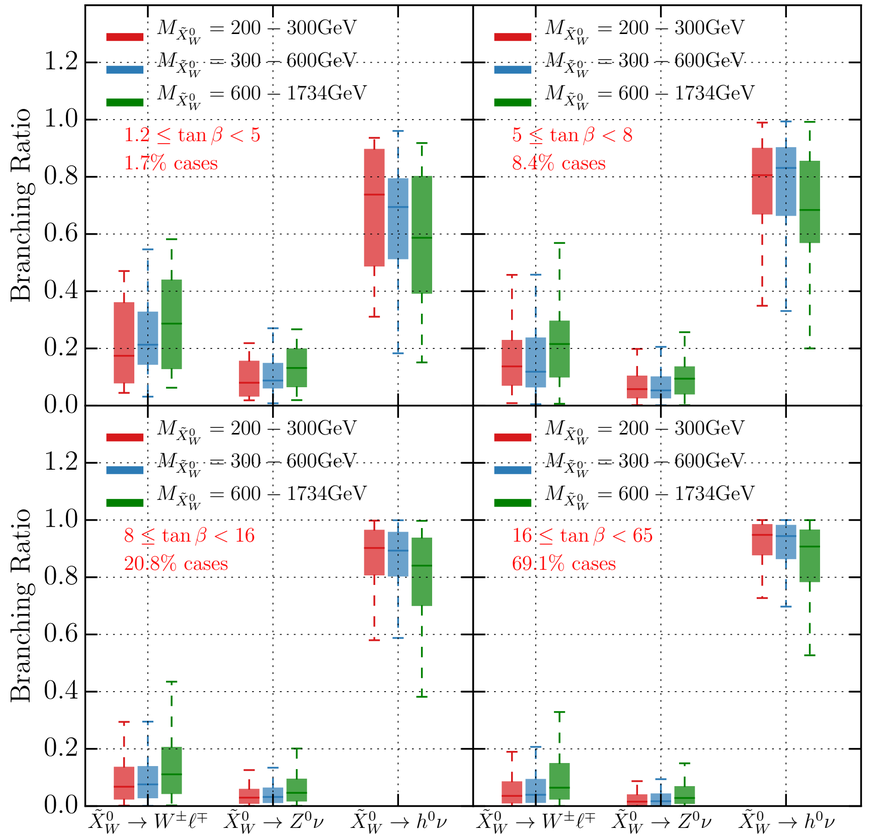

Figure 12: Branching ratios for the three possible decay channels of a Wino neutralino LSP divided over three mass bins and four $\tan\beta$ regions. The colored horizontal lines inside the boxes indicate the median values of the branching fraction in each bin, the boxes indicate the interquartile range, while the dashed error bars show the range between the maximum and the minimum values of the branching fractions. The case percentage indicate what percentage of the physical mass spectra have $\tan\beta$ values within the range indicated. We assumed a normal neutrino hierarchy, with $\theta_{23} = 0.597$.

each of these, we compute the decay rates via RPV processes, using the expressions (E.2)-(E.8) with $n = 2$ given in Appendix E. The branching ratios of the main channels take different values for different valid points in our simulation. These values are scattered around the median values of these

arXiv:1811.05581

Setting Limits

- Limits are set across the full BR plane of possible wino decays, both boson type (Z, W, H) and lepton flavor (e,μ,τ)
- BRs can inform neutrino hierarchy
- We will also calculate a model-independent significance for each $m_{Z\ell}$ bin

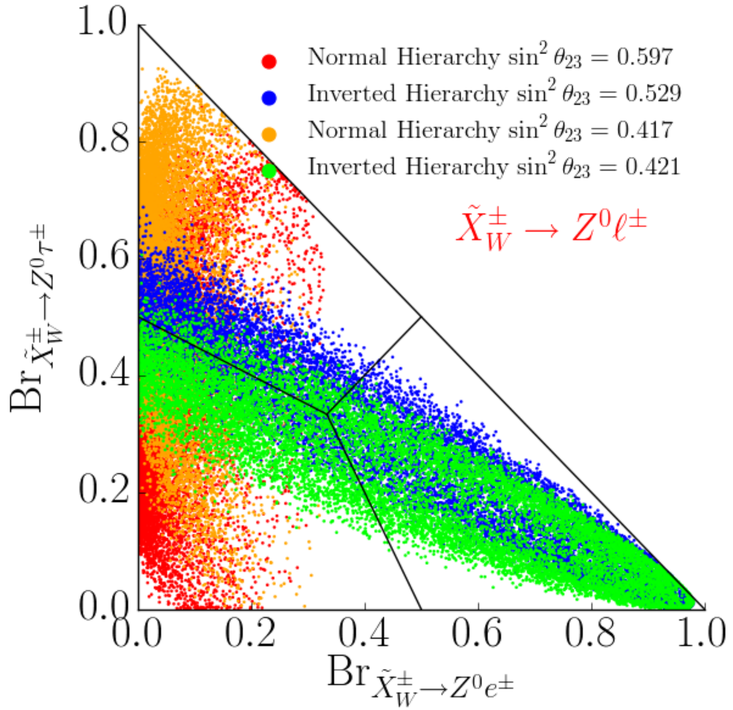

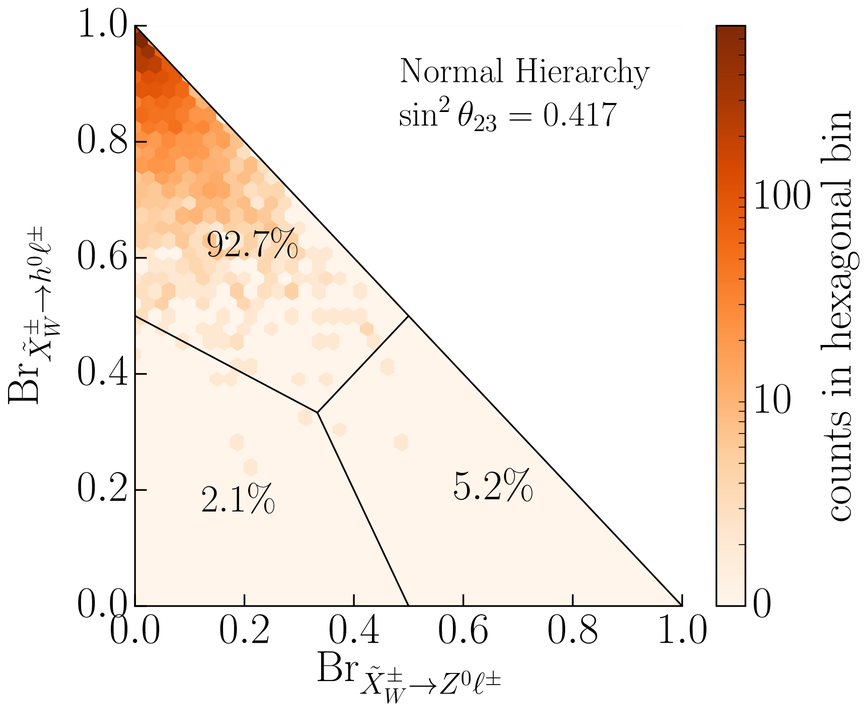

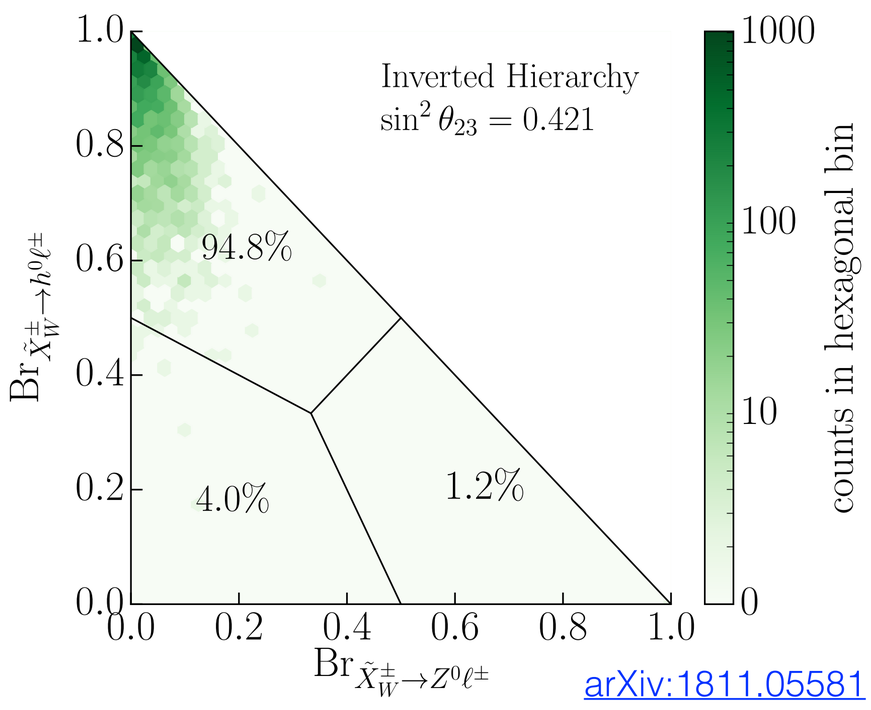

arXiv:1811.05581

Neutrino Hierarchy

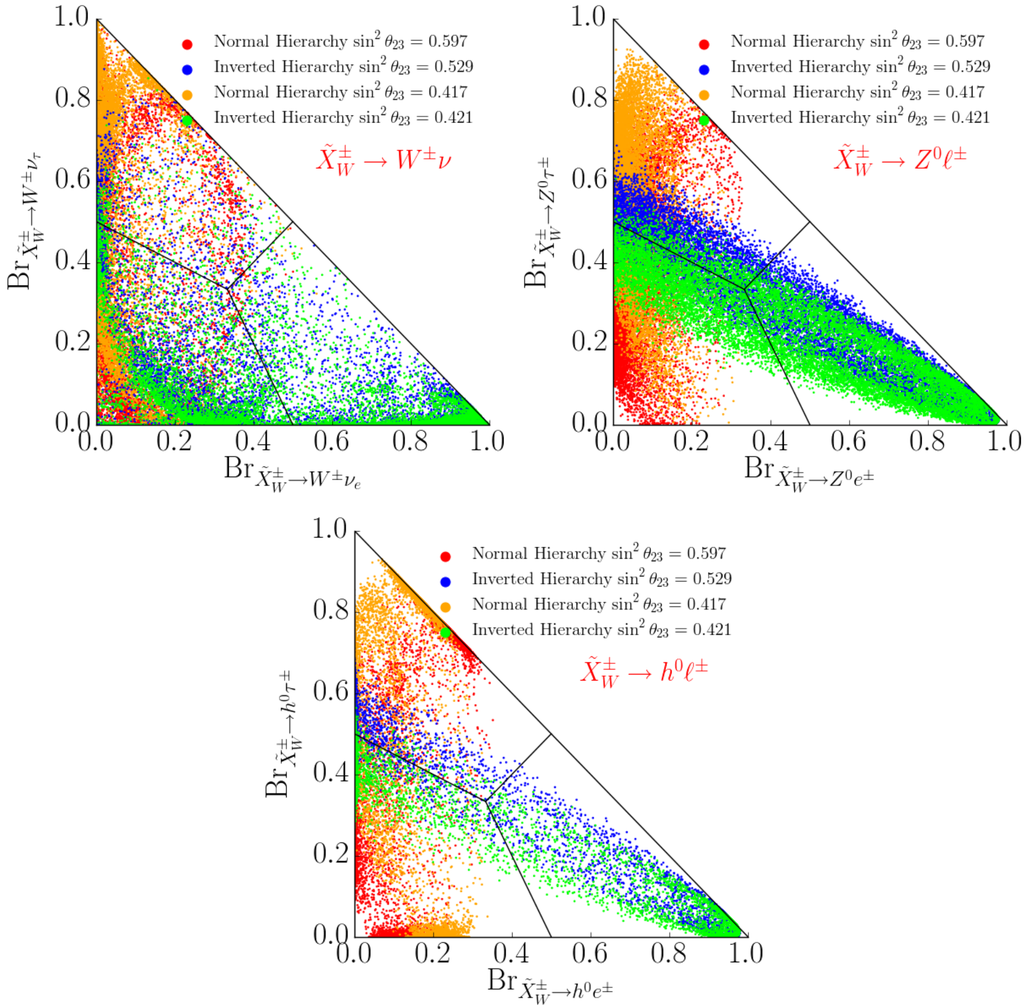

Figure 10: Branching ratios into the three lepton families, for each of the three main decay channels of a Wino chargino LSP. The associated neutrino hierarchy and the value of θ_{23} is specified by the color of the associated data point.

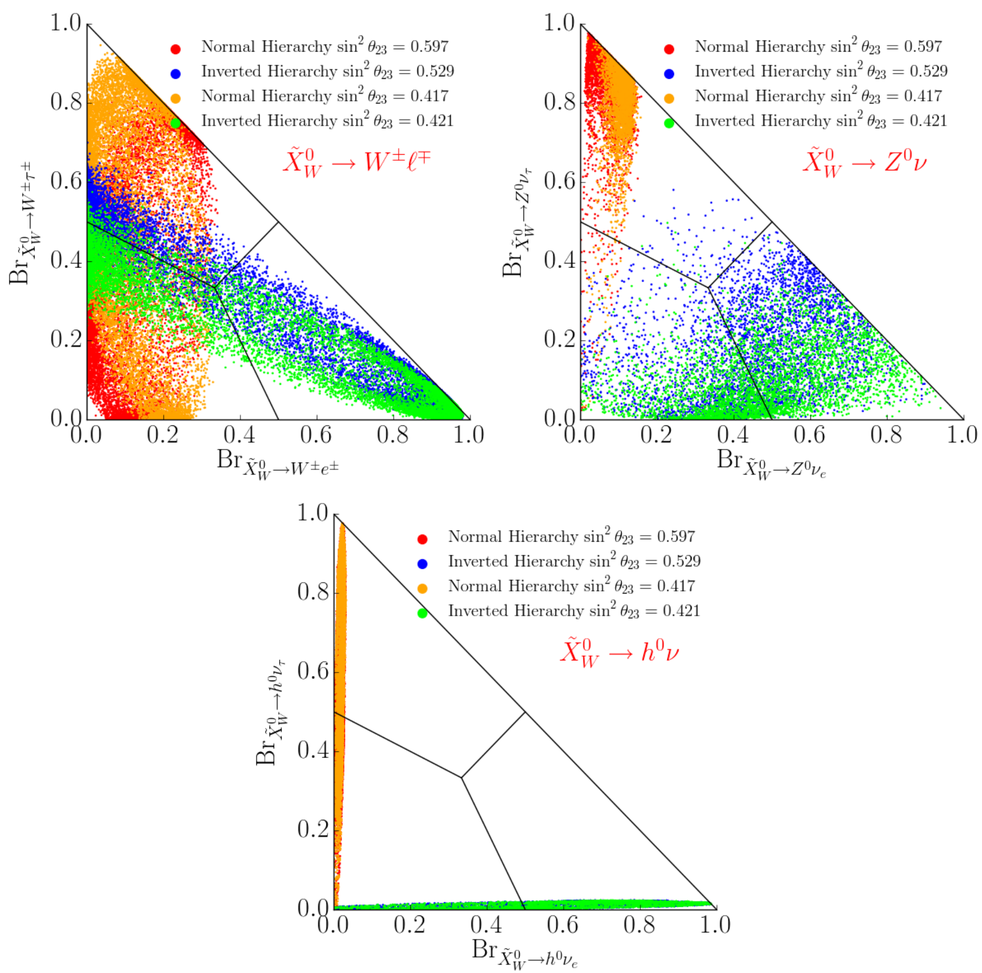

Figure 15: Branching ratios into the three lepton families, for each of the three main decay channels of a Wino neutralino LSP. The associated neutrino hierarchy and the value of θ_{23} is specified by the color of the associated data point.

arXiv:1811.05581

Statistical Scan of MSSM B-L RPV Model

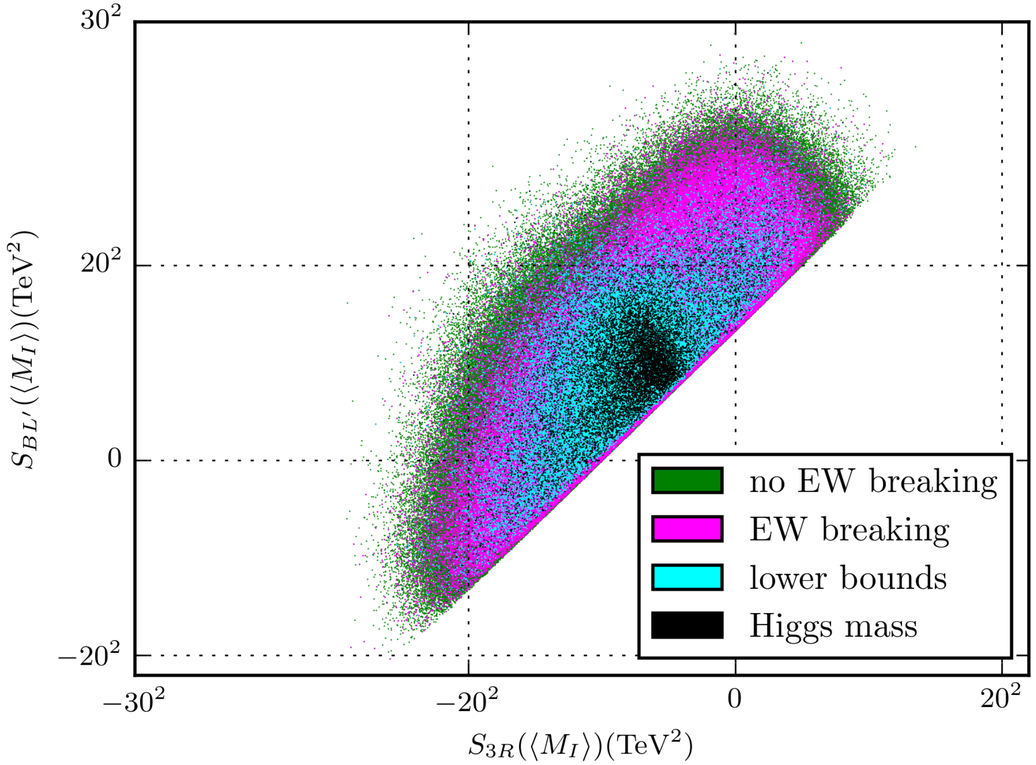

Figure 2: Plot of the 100 million initial data points for the RG analysis evaluated at M_I . The 4,351,809 green points lead to appropriate breaking of the $B-L$ symmetry. Of these, the 3,142,657 purple points also break the EW symmetry with the correct vector boson masses. The cyan points correspond to 342,236 initial points that, in addition to appropriate $B-L$ and EW breaking, also satisfy all lower bounds on the sparticle masses. Finally, as a subset of these 342,236 initial points, there are 67,576 valid black points which lead to the experimentally measured value of the Higgs boson mass.

arXiv:1810.11035

Long Lived?

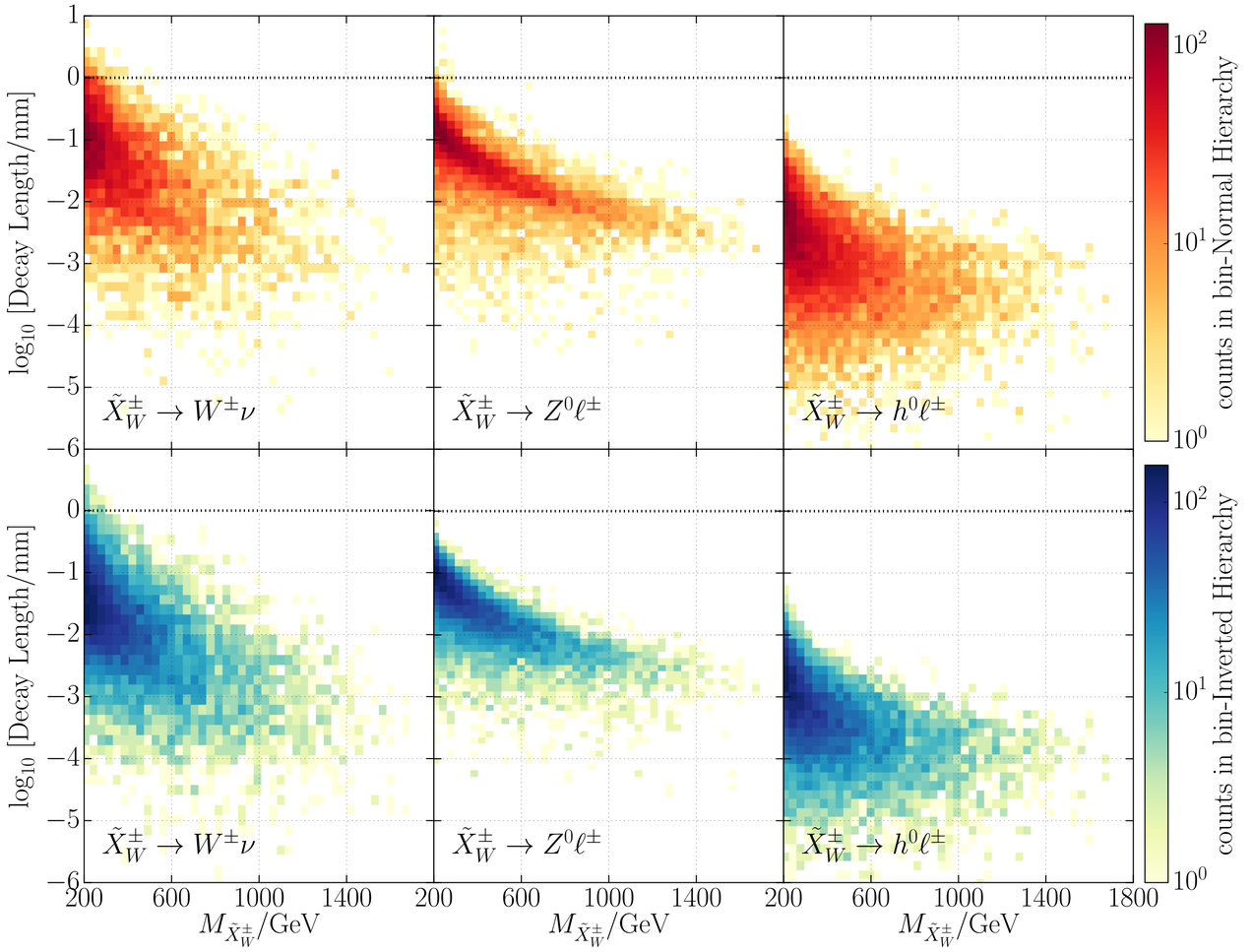

Figure 9: Wino Chargino LSP decay length in milimeters, for individual decay channels, for both normal and inverted hierarchies. We have chosen $\theta_{23} = 0.597$ for the normal neutrino hierarchy and $\theta_{23} = 0.529$ for the inverted hierarchy. The choice of θ_{23} has no impact on the decay lengths. All individual channels have decay lengths < 1mm

arXiv:1811.05581